Chapter One

General Introduction

1.1 Preface

Pin numbers, email passwords, credit card numbers, and protected premises access numbers all are sort of identities usually used to identify persons. Unfortunately, all these identities have some common shortcoming; i.e. they can easily be stolen or guessed. This leads to some logical problems: i.e. people tend to forget multiple, lengthy and varied passwords, therefore, they use one strong password for everything but, unlikely, this allows the successful thief to gain access to all the protected information. However, the written identities may be replaced with some of the physical traits used by biometric authentication programs; such as ***fingerprints and retinas***, other tests include the ***voice, face, or iris***. These technologies are now very real and are currently being used in a variety of private sectors [Pau04].

Iris recognition is the identification of a person's identity based on an image of their eye. This is done by analyzing the various patterns that makeup the iris. These patterns are ideal for biometric identification because they are both hard to alter as well as exceptionally complex. Another important feature of the iris is the great variability over many eyes. Each iris is unique (even the left and right eyes are different) and similar to fingerprints–iris patterns are not shared between identical twins [Jam03, Dau04].

1.2 Biometrics

Biometrics is the science of using digital technology to identify an individual, based on unique biological characteristics. Biometrics personal identification has been largely motivated by the increasing requirement for security in a networked society [Lib03, Li04].

In many accesses control applications such as: border control, immigration, airports, and other high security environments, biometrics authentication and security methods are more appropriate to prevent unwanted intrusion and to protect an individual's privacy, because of using measurable biological features of an individual to authenticate his/her identity. One of these methods is iris recognition method [Hib03].

A good biometric is characterized by use of features that are; highly unique, so that the chance of any two people having the same characteristic will be minimal; stable; i.e. the features do not change over time, easily captured in order to provide convenience to the user, and prevent misrepresentation of the feature [Lib03]. In fact, the indicated stability conditions are biological behaves which could be classified as [Chr00]:

1. Physiological characteristics: including fingerprint, hand geometry, eye (iris and retina) patterns, and facial features.
2. Behavioral characteristics: including voice and signature.

Biometrics, which refers to identify individual physiological or behavioral characteristics, has the capability to reliably distinguish between an authorized person and an imposter [Li02a].

Generally, physiological and behavioral characteristics used in biometric measurements. These measurements provide a robust approach to a wide range of applications; e.g. identity authentication and access control. Among all these patterns, iris recognition is a more recent method for personal identification [Li02a].

Today, biometrics authentication methods are widely used in the areas that need to be highly secure; e.g. banks, computer networks, government, and law enforcement agencies. Current biometrics methods involve the following [Hib03]:

1. ***Eye Scanning:*** it can be divided into two different fields:
   - ***Iris scanning:*** measures the texture components of the tissue surrounding the pupil of the eye.
   - ***Retina scanning:*** directing a low intensity beam of light through the pupil (to the back of the eye) to measure the pattern of blood vessels at the back region of the eye.
2. ***Face Recognition:*** analyzes the unique shape, pattern and positioning of facial features.
3. ***Fingerprint Scanning:*** the series of ridges and furrows on the surface of the finger as well as the minutiae points are measured and identified.
4. ***Hand Geometry:*** measures the shape and length of fingers and knuckles.
5. ***Finger Geometry:*** the geometric and shape of the fingers are considered to identify and recognize the owner person.
6. ***Signature Recognition:*** it measures the manner in which users signs their names (e.g. stroke order, speed, pressure), and other factors which relate to the actual behavior of signing a document.

1.3 The Structure of Human iris

The iris is a thin circular diaphragm in the eyeball that surrounds the pupil, it lies between the cornea and the lens of the human eye and consists of the muscles that adjust the size of the pupil. Formation of the iris begins during the third month of embryonic life, and remains unchanged for the rest of person's life, so iris recognition realizes a high level of security. Figure (1.1) shows the structure of the human eye [Li04, Jam03].

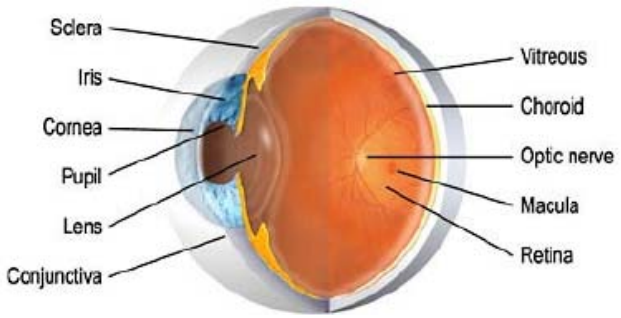

Figure (1.1) The structure of the human eye

The iris consists of a number of layers; the lowest is the epithelium layer, which contains dense pigmentation cells. The stromal layer lies above the epithelium layer, and contains blood vessels, pigment cells and the two iris muscles. The density of stromal pigmentation determines the color of the iris [Li04, Jam03].

Figure (1.2) illustrate a fronton view of the human eye, the externally visible surface of the multi-layered iris contains two zones, which often differ in color. An outer ciliary zone and an inner pupillary zone, and these two zones are divided by the collarette which appears as a zigzag pattern [Lib03, Ger97].

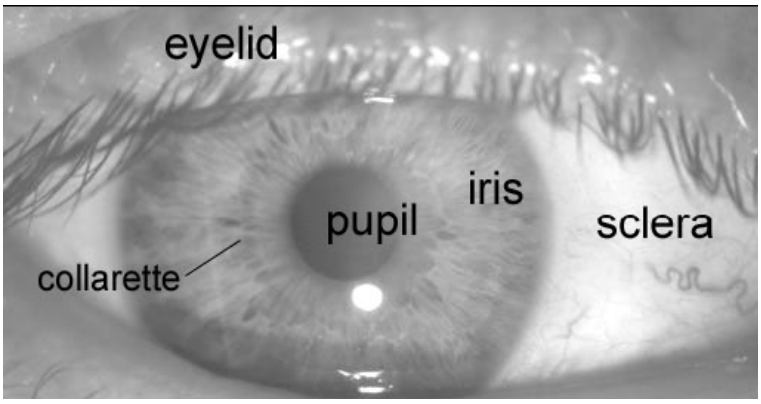

Figure (1.2) A fronton view of the human eye

Formation of the unique patterns of the iris is random and not related to any genetic factors. The only characteristic that is dependent on genetics is the pigmentation of the iris, which determines its color. Due to the epigenetic nature of iris patterns, the two eyes of an individual contain completely independent iris patterns; this even applies to identical twins [Lib03, Jam03].

1.4 Features of the Iris

The human iris is rich in features which can be used to quantitatively and positively distinguish one eye from another. The iris contains many collagenous fibers, contraction furrows, coronas, crypts, color, serpentine vasculature, striations, freckles, rifts, and pits. Measuring the patterns of these features and their spatial relationships to each other provides other quantifiable parameters useful to the identification process. Despite of its delicate nature, the iris is protected behind eyelid, cornea, aqueous humor, and frequently eyeglasses or contact lenses (which have negligible effect on the recognition process). Some of these feature [Ger97]:

1.4.1 Stability and Reliability of the iris

The iris is a protected internal organ in the body whose random texture is stable throughout life. Compared with other biometric features such as face and fingerprint, iris patterns are more stable and reliable from about one year of age until death, meaning that the patterns on the iris are relatively constant over a person's lifetime, because it is not subjected to the environment, as it is protected by the cornea and aqueous humor [Jes05, Yin04a].

1.4.2 The Uniqueness of the Iris

The iris is unique because of the chaotic morphogenesis of that organ [Lib03, Ger97]. To recognize the uniqueness of the iris, the iris must be analyzed; there must be bits of an iris code that are statistically independent. Statistically independent means an event's likelihood of occurrence is equally probable regardless of the outcome of a given event. For example, in DNA testing between a pair of identical twins, (twins from the same embryo), yield the same results, that they have four unique irises. Thus, an iris image is unique and independent of an identical genetic makeup [Jes05, Dau01].

1.5 Applications of Iris Recognition

The major applications of this technology so far have been: substituting for passports (automated international border crossing), aviation security and controlling access to restricted areas at airports, database access and computer login, access to buildings and homes database searching at border crossings, and other government programmers [Dau94].

Iris recognition has proven to be a very useful and versatile security measure; and it will prove to be a widely used security measure in the future as shown below [Jes05]:

Airports: A recent application of iris recognition has been in the transportation industry, most notably airline travel. The security advantages given by iris recognition software have found to yield a strong potential to fix problems in transportation. The iris recognition machines expedite the process of passengers going through airport security, allowing the airports to run more efficiently. It is also used for immigration clearance, airline crew security clearance, airport employee access to restricted areas, and as means of screening arriving passengers for a list of expelled persons from a nation [Jes05].

Gate Systems: Systems that use iris recognition reference each individual's unique iris code, so it is possible to maintain an extremely high level of security. Since it is also possible to basically check one's identity without making contact by using an infrared camera, there are no unpleasant feelings like there are when giving fingerprints [Jes05].

1.6 Aim of the Thesis

The aim of the thesis is to design a computer system that can recognize, verify, differentiate, and identify persons from their iris images.

1.7 Literature Survey

There are some researchers investigated the subject of the iris where from identifying, verifying, classifying and matching. From those literatures:

- **[Dun95], "Optimal Gabor Filters for Texture Segmentation":** In this work, texture segmentation involves subdividing an image into differently textured regions based on a filter-bank model, called Gabor filters. The goal is to transform texture differences into detectable filter-output discontinuities at texture boundaries. By locating these discontinuities, one can segment the image into differently textured regions. They argue that Gabor filter outputs can be modeled as random variables and develop a decision-theoretic algorithm for selecting optimal filter parameters. Experimental results indicate that the method is superior to previous methods in providing useful Gabor filters for a wide range of texture pairs.

- **[Tai96], "Image Representation Using 2D Gabor Wavelets":** This paper extends to two dimensions, the frame criterion for one-dimensional 1D wavelets, and it computes the frame bounds for the particular case of two-dimensional 2D Gabor wavelets. The conditions have been derived under which a set of continuous 2D Gabor wavelets will provide a complete representation of any image, and also find self-similar wavelet parameterizations which allow stable reconstruction by summation as though the wavelets formed an orthonormal basis. Approximating a "tight frame" generates redundancy which allows low-resolution neural responses to represent high-resolution images.

- **[Ger97], "Iris Recognition Technology":** He used Iridian technologies, this new technology, using the unique patterns of the human iris, overcomes previous shortcomings and provides positive recognition of an individual without contact or invasion, at extremely high confidence levels. The video-based system locates the eye and iris, evaluates the degree of occlusion by eyelid and specular reflection, determines the quality of image focus, and determines the center and boundary of the pupil and the limbus (outer edge of the iris) for processing. The features of the iris are then measured and encoded into a 512 byte IrisCode record for enrollment or recognition. The resulting IrisCode record is compared to each IrisCode record enrolled in the database for recognition.

- **[Dau01], "Epigenetic Randomness, Complexity, and Singularity of Human Iris Patterns":** In a similar analysis done by Daugman, 648 iris images from 324 people were subjected to the same conditions used to render a Hamming distance. The mean and standard deviation for this analysis were 0.497 and 0.031, respectively. This study was repeated with the irises from identical twins and yielded a similar result. These studies show that an individual has two unique irises, and a pair of twins has four unique irises. Thus, an iris image is independent of an identical genetic makeup.

- **[Li02a], "Iris Recognition Using Circular Symmetric Filters":** This work proposes a new method for personal identification based on iris recognition. A bank of circular symmetric filters is used to capture local iris characteristics to form a fixed length feature vector. In iris matching, an efficient approach called Nearest Feature Line (NFL) is used. Constraints are

imposed on the original NFL method to improve performance. Experimental results show that the proposed method has an encouraging performance.

- **[Jam03], "Statistical Pattern Recognition of the Iris":** This work involved pattern recognition techniques to recognize the identity of a person based on (his/her) iris. Preprocessing is done on the image to extract an Iris Map which contains a normalized image of the data in the annular region defined by the boundaries of the iris. Synthetic data is generated from the Iris Map, and then collected for feature extraction by sampling the iris in 50-pixel increments at concentric circles. A windowed fourier transform is then performed on the resulting data, the power vectors are then segmented into eight observables using vector quantization, to generate an observations sequence.

- **[Bho04], "Personal Identification Based on Iris Patterns":** The work presented in this paper involved developing and implementing an iris recognition system. For determining the performance of recognition system, a database of grayscale eye images was used. Iris recognition system does the online verification by capturing iris images using a specially designed camera system and matches it with already stored iris code database. Two algorithms (circular-mellin and corner detection based algorithm) were fused to design an iris recognition system. The accuracy of the system is found to be 97 %.

- **[Ali05], "Fingerprints Recognition Using Gabor Filters":** This work is an attempt to recognize and identify fingerprint among many that were stored in data base, using bank of gabor filters. The introduced algorithm determines the automatically core point and the tessellate region of interest around the core point. The utilized bank of gabor filters have the ability to capture both local and global details in a fingerprint as a compact fixed length finger vector by computing the Average Absolute Deviation (AAD) from the mean of gray values in an individual sector in the filtered images. The matching process in this present system is based on the Euclidean distance between the new input fingerprint and templates stored in the data base. So the score degree can determine the genuine or imposter person.

- **[Hug06], "Iris Recognition: An Analysis of the Aliasing Problem in the Iris Normalization Stage":** In this paper, the relationship between the size of the captured iris image and the overall recognition's accuracy has been analyzed. Further, the threshold for the sampling rate of the iris normalization process which the error rates significantly increase has been identified. No significant degradation in the accuracy have been observed when the sampling rates are lower than 5. For higher sampling rates (correspondent to original images with iris area below 30% of the normalized one), the error rates significantly increase.

1.8 Thesis Layout

The reminder of this thesis is organized as follows:

1. ***Chapter Two: "Image Processing Methodologies",*** presents the associated image processing and pattern recognition techniques that are used to extract features from the iris image, by performing preprocessing stage and feature extraction stage.
2. ***Chapter Three: "Iris Recognition System Design",*** presents the description of the designed iris recognition and identification system.
3. ***Chapter Four: "Experimental Results and Discussion",*** presents the implementation and evaluation of the designed iris recognition system, results analysis, and database view.
4. ***Chapter Five: "Conclusion and Future works",*** it implies the conclusion of thesis and suggestions for future work.

Chapter Two

Image Processing Methodologies

2.1 Introduction

Image techniques are widely used for too many useful applications. One of the most important implementation of the image processing methods is in the field of pattern recognition. Recognition methods depend on performing several image techniques; i.e. image binarization, image edge detection, image transformation, chain coding, etc [Gon87]. In this chapter, the most related image techniques with the thesis topic will be discussed and investigated. As an introductory to this topic, the digital representation of images will be discussed first, and then the related digital techniques will be mentioned.

2.2 Digital Image Representation

A digital image can be described as combination of Discrete Numbers (DN), arranged in matrix form (columns and rows), each (DN) called image element and briefly referred as pixel. An image array of size M×N is presented by:

$$f(x,y) = \begin{bmatrix} f(0,0) & f(0,1) & \cdots & f(0,N-1) \\ f(1,0) & f(1,1) & \cdots & f(1,N-1) \\ \vdots & \vdots & \cdots & \vdots \\ f(M-1,0) & f(M-1,1) & \cdots & f(M-1,N-1) \end{bmatrix} \quad \ldots\ldots\ldots (2.1)$$

Where *f(i,j)*, i = 0, 1, 2, … *M*-1, and j = 0, 1, 2, … *N*-1, represents the brightness at the point of coordinates (i,j). The range of assigned on each elements defined the type of the image (i.e. binary, grayscale, or color) [Umb98, Gon87].

2.3 Types of Digital Images

Digital images are presented in different types, depending on the requiring area. For examples, simple binary image are useful for recognition process, while grayscale image is required to visualized the differences between image regions, colored images are mostly used to globalize the faint regions, and superficial the image behavior. However, multi-spectral images have specific implementations (usually used for remote sensing applications), as described below [Umb98]:

2.3.1 Binary Images

Is simplest type of images which take values, typically black and white, or '0' and '1'. A binary image is referred to as a 1 bit/pixel image because it takes only 1 binary digit to represent each pixel. This type of image is most frequently used in computer vision applications where the only information required for the task is general shape, or outline information. Binary images are often created from grayscale images via a threshold operation, where every pixel above a decided threshold given value '1', and those below it given '0'.

2.3.2 Grayscale Images

They are referred to as monochrome, or one-color, images. They contain brightness information only. The number of bits used for each pixel determines the number of different brightness levels available. The typical image contains 8 bits/pixel data, which allows us to have 256 (0-255) different brightness (gray) levels, see fig (2-1a).

Additionally, the 8-bits representation is typical due to the fact that the byte, which corresponds to 8 bits of data, is the standard small unit in the world of digital computers.

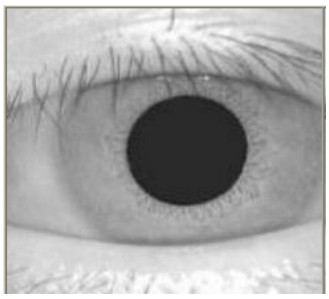

Figure (2.1) A grayscale eye's image

2.3.3 Color Images

Color images can be modeled as three-band monochrome image data, where each band of data corresponds to a different color. The actual information stored in the digital image data is the brightness information in each spectral band. When the image is displayed, the corresponding brightness information is displayed on the screen by picture elements that emit light energy corresponding to that particular color. Typical color images are represented as Red, Green, and Blue, or RGB images. Using 8-bit monochrome standard as model, the corresponding color image would have 24 bits/pixel, 8-bits for each of the three-color bands (red, green, and blue).

2.3.4 Multi-spectral Images

Multi-spectral images typically contain information outside the normal human perceptual range. This may include infrared, ultraviolet, X-ray, acoustic, radar or other remote sensed images. These are not images in the usual sense because the information represented is not directly visible by the human system. However, the information is often represented in visual form by mapping the different spectral bands to RGB components.

2.4 Image Processing Techniques

Image processing is computer imaging where the application involves a human being in the visual loop. In other words, the images are to be examined and acted upon by people [Gon87, Umb98]. For these types of applications, some understanding of how the human visual system operators have been required. The major topics within the field of image processing include:

2.4.1 Image compression

Image compression involves reducing the typically massive amount of data needed to represent an image. This is done by eliminating data that are visually unnecessary and by taking advantage of the redundancy that is inherent in most images.

2.4.2 Image restoration

Image restoration is the process of taking an image with some known, or estimated, degradation, and restoring it to its original appearance. It's often used in the field of photography or publishing where an image was somehow degraded but needs to be improved before it can be printed.

2.4.3 Image enhancement

One of the simplest and often most dramatic enhancement techniques is to simply stretch the contrast of an image. It's used to make an image look better, by using knowledge of the human visual system's response to improve an image visually; e.g. image smoothing and image sharpening.

2.5 Pattern Recognition System

A pattern defines "as opposite of a chaos; it is an entity, vaguely defined, that could be given a name". For example, a pattern could be a fingerprint image, a handwritten cursive word, a human face, iris recognition, or a speech signal [Ani00].

Recognition is regarded as a basic attribute of human beings, as well as other living organisms. Automatic (machine) recognition, description, classification, and grouping of patterns are important problems in a variety of engineering and scientific disciplines such as biology, psychology, medicine, marketing, computer vision, artificial intelligence, and remote sensing [Gon74]. The techniques involved in the branch of images processing field will be considered in details through this present work, because they represent the core of this thesis.

2.5.1 Basic Concepts of Pattern Recognition

A human being is very sophisticated information at system, partly, because he possesses a superior pattern recognition capability. According to the nature of the patterns to be recognized, recognition may be divided into two major types: the recognition of *concrete items* and the recognition of *abstract items*. The concrete items recognize characters, pictures, music, and the objects around us. This recognition process involves the identification and classification of spatial and temporal pattern.

Examples of spatial patterns are characters, iris, fingerprints, weather maps, physical objects, and pictures. Temporal patterns include speech waveforms, electrocardiograms, target Signatures, and time series. On the other hand, the abstract items recognize an old argument, or a solution to a problem, with our eyes and ears closed [Ali05b].

The study of pattern recognition problems may be logically divided into two major categories:

1. The study of the pattern recognition capability of human beings and other living organisms.
2. The development of theory and techniques for the design of devices capable of performing a given recognition task for a specific application.

While the first subject area is concerned with such disciplines as psychology, physiology, and biology, the second area deals primarily with engineering, computer, and information science [Ali05b]. This work is concerned with the computer.

2.5.2 Typical Pattern Recognition System

The typical pattern recognition process is shown in figure (2.2). The operations of input data are referred as preprocessing operations. The preprocessing step includes a number of image processing operations that transform the input image into another form. After proper preprocessing, several pattern features are extracted in a pattern vector which is plotted in the pattern space, called feature extraction step. While the proper decision theory sketches the optimum boundaries in the space of the recognition during the classification step [Gon74].

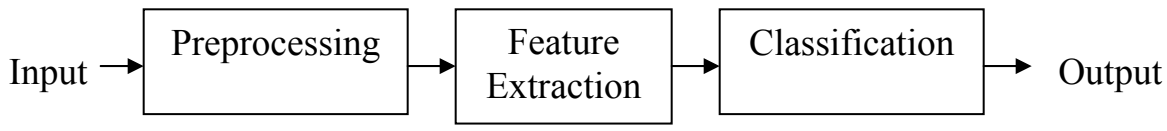

Figure (2.2) Block diagram of typical pattern recognition system

2.6 Processes of typical pattern recognitions

Some of the most common operations involved in each of the typical pattern recognition processes are:

2.6.1 Preprocessing Operation

Generally, the preprocessing operations involve all these procedures that are performed to simplify the image format and make it ready to generate simple, clear, understandable features. These operations may involve different image processing methods; e.g. image partitioning into small blocks, image binarization by implementing certain threshold or by utilizing certain edge detector, image enhancement methods (to remove the undesired redundancies or to globalize the image features etc.). Here, only pre-operations required for this recognition system should be discussed; i.e.:

A. ***Image De-Colorization Preprocess***

Mostly, eye images are presented in colored form (i.e. RGB bands). In this present designed recognition system and, for simplification, the processed images are adopted to be in a grayscale form.

Therefore, all accessed colored images to the system have been converted into grayscale version, simply by averaging, pixel-to-pixel, the RGB image bands. Eq.(2.2) illustrates the color conversion operation that given by [Gon87]:

$$Gray_{-image}(x,y) = \frac{\mathrm{Re}\,d_{-Band}(x,y) + Green_{-Band}(x,y) + Blue_{-Band}(x,y)}{3} \quad \ldots\ldots (2.2)$$

B. Edge Detection Process

It's an important task in image processing; it is used as a preprocessing step in many enhancement and image processing applications. An edge can be defined as "the boundary between two regions with relatively distinct gray-level properties". There are many different operators, which yield high values in the region where brightness is changing rapidly, are usually used to detect edges [Gon87], such as 1st order of the intensity; this gives us the intensity gradient of the original data i.e. Sobel, Prewitt, Kirstch, and Roberts, and 2nd order i.e. Laplacian of Gaussian (LoG), zero-crossing operators of the second order derivative in the gradient direction [Csa07, Har05].

Despite of the ease of the 1st order mentioned edge methods, and certain disadvantages associated with its results; i.e. using low threshold value produces thick boundaries (because not only the true edge points will be detected but, also, the neighbor points to the true edges). However, increasing threshold value may produce undesired open boundaries (i.e. gaps between edge lines) [Kas94]. All these effects are not desirable in this recognition system because, regions extraction will be difficult.

To overcome the threshold utilizing problems, and provides close contour and single edge, other more advance edge detection technique should be used; i.e. Marr-Hildreth method.

Marr-Hildreth algorithm for edge detection is based on the zero-crossings of the Laplacian of the Gaussian operator. Edges are found at zero-crossings of the resulting image [Har05]. The procedures involved in this method can be summarized by the following points:

I. To detect edges in an image with a relatively large-scale of intensity changes, some forms of image intensity smoothing must first be carried out to reduce the range of scale over which intensity changes take place, that an optimal smoothing can be performed by convolving the discrete image array *img(x, y)* with a two-dimensional Gaussian operator "*G*(*x, y*)", given by:

$$A(x,y) = G(x,y) \otimes img(x,y) \qquad \ldots\ldots\ldots\ (2.3)$$

Where, *A(x,y)* is the smoothed image array, and

$$G(x,y) = \frac{1}{2\pi\sigma\ x\sigma\ y} e^{-[\frac{x^2+y^2}{2\sigma x^2}]} \qquad \ldots\ldots\ldots\ (2.4)$$

II. Performing the Laplacian operation:

$$\nabla img(x,y) = \frac{\partial img(x,y)}{\partial x} + \frac{\partial img(x,y)}{\partial y} \qquad \ldots\ldots\ldots\ (2.5)$$

Where $\frac{\partial}{\partial x}$ and $\frac{\partial}{\partial y}$ representing the 1st order partial derivatives of $\frac{d}{dx}$, and the 2nd order partial derivatives of $\frac{d}{dx}$ represented by:

$$\nabla^2 img(x,y) = \frac{\partial^2 img(x,y)}{\partial x^2} + \frac{\partial^2 img(x,y)}{\partial y^2} \qquad \ldots\ldots\ldots\ (2.6)$$

Marr and Hildreth found that using only the second derivative (i.e. Laplacian operator ∇^2) leads to a great saving in computational time. The two operators (i.e. Laplacian and Gaussian) can be combined into one operator denoted by "$\nabla^2 G$" and cal1ed *Marr-Hildreth* operator [Kas94, Har05].

$$\nabla^2 G = \nabla^2 (x, y) \otimes G(x, y) \quad \ldots\ldots (2.7)$$

III. The last step of the detection is searching for the zero-crossing in the second derivative of the image, by assigning all zero-crossing points as to be edge points. This is done by searching for the change in signal sign of each point in the 4-neighbors (i.e. scanning the signal pixel by pixel for the zero-crossing points). Moreover, only one side of zero-crossing is marked, specifically the negative side as shown in eq.(2.8). As a result one pixel thick boundaries will be produced [Kas94].

$$\begin{aligned} &\text{If } \textit{pre-value} * \textit{post-value} < 0 \quad \text{Then} \quad \textit{img(x, y)} = 1 \\ &\text{or, If } \textit{up-value} * \textit{down-value} < 0 \quad \text{Then} \quad \textit{img(x, y)} = 1 \quad \ldots\ldots \quad (2.8) \end{aligned}$$

The only threshold value used in this technique, which can affect its performance, is the width of the Gaussian operator represented by the standard deviation value σ, that given in eq.(2.8).

C. Thresholding

This technique is based on a simple concept. A brightness parameter (*Thr*) which is called the brightness threshold is chosen and applied to the image *img(x, y)* according to the following criterion:

If $img(x, y) > Thr$ then $img(x, y)$ = object = 1

Else $img(x, y)$ = background = 0

This kind of thresholding implies the interested in light objects on a dark background. For dark objects on a light background, the following criterion would be used:

If $img(x, y) < Thr$ then $img(x, y)$ = object = 1

Else $img(x, y)$ = background = 0

The output is the label "object" or "background" which, due to its dichotomous nature, can be represented as a boolean variable "1" or "0". While there is no universal procedure for threshold selection that is guaranteed to work on all images, there are a variety of alternatives; one of them is the fixed thresholding [Umb98]. Fixed thresholding can be defined as an alternative to use a threshold value that is chosen independently of the image data [Hib03].

D. Convolution

The convolution of two function $f(x)$ and $g(x)$, denoted by $f(x) \otimes g(x)$ is defined by the integral [Gon87]:

$$f(x) \otimes g(x) = \int_{-\infty}^{\infty} f(\alpha) g(x - \alpha) dx \quad \ldots\ldots \quad (2.9)$$

Since the mechanics of the convolution integral are not particularly easy to visualize, convolution process was adopted.

When the convolution process performed in LoG operator as it's mentioned before, large size of LoG operator required a large number of multiplication and addition operations. Consequently, the edge detector will be slow. So, for faster

implementation, the convolution is usually performed by utilizing the Fourier Transformation (FT); i.e.

$$f(x) \otimes g(x) = \Im^{-1}\{F(u)G(u)\} \quad \ldots\ldots\ldots (2.10)$$

Where *F(u)* and *G(u)* are the Fourier Transform of the functions *f(x)* and *g(x)*, respectively. $\Im^{-1}\{F(u)G(u)\}$, indicating the Inverse Fourier Transform (IFT) process.

For an N×N image, the equation for the 2D discrete fourier transform is]:

$$F(u,v) = \frac{1}{N}\sum_{x=0}^{N-1}\sum_{y=0}^{N-1} f(x,y)\exp^{-j2\pi\frac{ux+vy}{N}} \quad \ldots\ldots (2.11)$$

Where *j* is the imaginary coordinate for a complex number, equals $\sqrt{-1}$.

After performing the transform, an IFFT given by eq.(2.12) are used to get the original image back.

$$\Im^{-1}[F(u,v)] = f(x,y) = \frac{1}{N}\sum_{u=0}^{N-1}\sum_{v=0}^{N-1} f(u,v)\exp^{j2\pi\frac{ux+vy}{N}} \quad \ldots (2.12)$$

Where $\Im^{-1}[]$ notation represents the inverse fourier transform process. As it's obvious, the difference between the forward and inverse operation is the +/- singe at the exponential term [Umb98, Jas03].

E. Chain coding Process

Chain coding is used to represent a boundary by a connected sequence of straight line segments of specific length and direction. Typically, this representation is based on 4 or 8 directions, each segment is coded by using a numbering scheme such as the ones shown in figure (2.3) [Gon87]:

Figure (2.3) Directions indexing for (a) 4-direction chain code, (b) 8-direction chain code

The basic information that store about a region is where it is. One could store the location of each pixel in the region, but one can be more efficient by simply storing the border. By traversing the border in a predefined direction around the region, one can build a *chain* [Ali05a].

2.6.2 Feature Extraction Operation

Any object or pattern which can be recognized and/or classified possesses a number of discriminatory properties or features. The first step in any recognition process performed either by a machine or by a human being, is to consider the problem of what discriminatory features to select and how to extract (measure) these features.

It is evident that the number of features to successfully perform a given recognition task depends on the discriminatory qualities of the chosen features. It is evident that the feature extraction plays central role in pattern recognition. In fact, the selection of an appropriate set of features which take into account the difficulties present in the extraction or selection process, and at the same time result in acceptable performance, is one of the most difficult task in the design of pattern recognition system [Gon74].

In this thesis feature extraction method will be performed to select the necessary and, as possible, invariant features for each processed iris image; i.e. Gabor filtering, image normalization and extract the iris region, etc.

The extracted features will be transferred into suitable vector form, and preserved in the constructed database library. A feature vector is composed of an ordered enumeration of the features extracted from the (local) information contained in each sub image (sector). The local discriminatory information in each sector needs to be decomposed into separate components. Gabor filter banks are a well-known technique to capture useful information in specific band-pass channels as well as to decompose this information into bi-orthogonal components in terms of spatial frequencies. A feature vector, which calls Iris-Code, is a collection of all the features (for every sector) in each filtered image. These features capture both the global pattern of ridges and valleys and the local characteristics. Matching is based on the minimum distance between the Iris-Codes.

A. Iris Localization

After the core point is determined, a given region should be extracted by defining its radius, since the pupil is generally darker than its surroundings, the iris region in an image can approximately be found by computing the average radius, then the iris region will be detected. The average radius computed by eq. (2.13) [Yin04a, Yon99].

$$R_{Average} = \frac{\sum_{i=1}^{end\ of\ contour} \sqrt{(x_i - \bar{x})^2 + (y_i - \bar{y})^2}}{\text{Number of contour points}} \qquad \ldots\ldots\ldots (2.13)$$

Where $(\bar{x}, \bar{y})$ denote the center coordinates of the pupil in theoriginal image *img(x, y)*.

B. Gabor Filters

To understand the concept of Gabor filtering, Gabor wavelets must be described first. Gabor wavelets are formed from two components; a complex *sinusoidal carrier* and a *Gaussian envelope* as shown in figure (2.4). The Gaussian envelope takes the form:

$$g(x, y) = s(x, y)\, w_r(x, y) \qquad \ldots\ldots\ldots (2.14)$$

The complex carrier takes the form:

$$s(x, y) = e^{j(2\pi(u_0 x + v_0 y) + p)} \qquad \ldots\ldots\ldots (2.15)$$

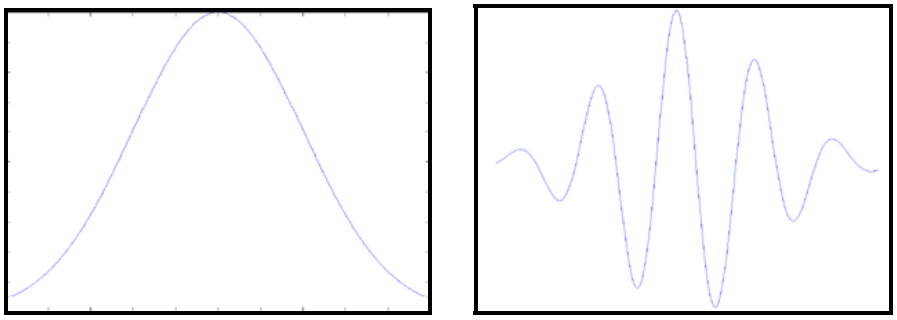

(a)Gaussian Envelope **(b)1D Gabor Wavelet**

Figure (2.4) Gaussian Envelope and 1D Gabor Wavelet

The real and imaginary parts of this function can be visualized, separately, as shown in this figure.

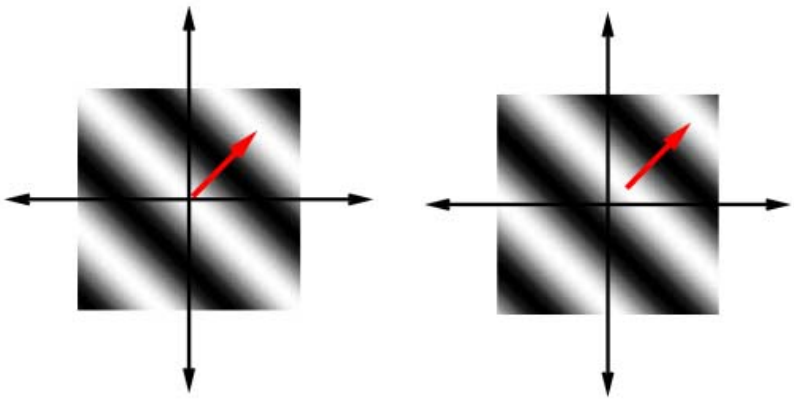

(a) **(b)**

Figure (2.5) Image Source1 (a) Real Part (b) Imaginary Part

The real part of the function is given by:

$$\text{Re}\,(s\,(x, y)) = \cos\,(2\pi\,(u_0 x + v_0 y) + P) \qquad \ldots\ldots\ldots (2.16)$$

And the imaginary:

$$\text{Im}(s\,(x, y)) = \sin\,(2\pi\,(u_0 x + v_0 y) + P) \qquad \ldots\ldots\ldots (2.17)$$

The parameters u_0 and v_0 represent the frequency of the horizontal and vertical sinusoids respectively. P represents an arbitrary phase shift.

The second component of a Gabor wavelet is its envelope. The resulting wavelet is the product of the sinusoidal carrier and this envelope. The envelope has a Gaussian profile and is described by the following equation [Dav04]:

$$g(x, y) = Ke^{-\pi(a^2(x-x_0)r^2 + b_2(y-y_0)r^2)} \quad \ldots\ldots\ldots (2.18)$$

where:

$$(x-x_0)_r = (x-x_0)\cos(\theta) + (y-y_0)\sin(\theta) \quad \ldots\ldots\ldots (2.19)$$

$$(y-y_0)_r = -(x-x_0)\sin(\theta) + (y-y_0)\cos(\theta) \quad \ldots\ldots\ldots (2.20)$$

The parameters used above are K-a scaling constant (a, b) - envelope axis scaling constants, θ - envelope rotation constant, (x_0, y_0) - Gaussian envelope peak. To put it all together, we multiply s(x, y) by w_r (x, y), this produces a 1D Gabor wavelet [Dav04].

Iris recognition is flow-like pattern which consist of locally parallel ridges and valleys. It has well-defined local frequency and local orientation. A set of band pass filters can efficiently remove the undesired noise and preserve the true ridge/valley structures [Ani91]. Gabor filters have both frequency-selective and orientation-selective properties and have optimal joint resolution in both spatial and frequency domains. Therefore, it is beneficial to use Gabor filters as band pass filters to remove the noise and preserve true ridge/valley structures [Ani91, Li02b].

An even symmetric Gabor filter has the following general form in the spatial domain [Ani91, Li02b]:

$$Gab(x, y; f, \theta,) = \mathrm{Exp}\left\{\frac{-1}{2}\left[\frac{x'^2}{\delta_{x'}^2}+\frac{y'^2}{\delta_{y'}^2}\right]\right\}\cos(2\pi f x') \qquad (2.21)$$

Where, $x' = x\cos\theta + y\sin\theta$, $y' = x\sin\theta - y\cos\theta$, and f is the frequency of the sinusoidal plane wave along the direction θ from the x axis, and $\delta_{x'}$ and $\delta_{y'}$ are the space constants of the Gaussian envelope along x' and y' axes, respectively (i.e. standard deviations of the Gaussian envelope).

C. Iris Normalization

Irises from different people may be captured in different size, and even for the iris from the same person, the size may change because of the variation of the illumination and other factors (the pupil is very sensitive to lighting changes). Such elastic deformations in iris texture affect the results of iris matching [Li02a, Yon99].

For the purpose of achieving more accurate recognition results, it is necessary to compensate for these deformations. Here, the normalization must used; it can reduce to a certain extent the distortion of the iris caused by pupil movement [Li02a].

For all the pixels in *Gimg(x, y)*, the normalized image is defined as:

$$N_i(x,y) = \begin{cases} M_0 + \sqrt{\dfrac{V_0 \times (img(x,y) - M_i)^2}{V_i}}, & \text{if } Gimg(x,y) >= M_i \\ M_0 - \sqrt{\dfrac{V_0 \times (img(x,y) - M_i)^2}{V_i}}, & \text{Otherwise} \end{cases} \quad \ldots. (2.22)$$

Where *Gimg(x, y)* denote the resulted image of Gabor function at pixel (*x, y*), M_i and V_i , the estimated mean and variance of *Gimg(x, y)*, respectively, and $N_i(x, y)$ is the normalized gray-level value at pixel (*x, y*). Normalization is a pixel-wise operation which does not change the clarity of the ridge and valley structures [Ani91].

2.6.3 Classification Operation

The most obvious way of establishing a measure of similarity between pattern vectors, is using distance function for classification operation. Pattern classification by distance function is one of the concepts in automatic pattern recognition. This simple classification technique is an effective tool for the solution of the problems in which pattern classes exhibit the reasonably limited degree of variability.

Several classifiers and recognition criteria can be attempted (i.e. minimum distance, maximum likelihood, etc.) to test the similarity between the preserved featured vector with any newly input one. The decision, then, decided according to the degree of the matching result [Gon74].

In this thesis, minimum distance is adopted and used to test the similarity between the preserved featured vectors with any newly input one.

The extracted feature vectors should fed to a matching process to determine the identity of the claimed user whose iris image is taken. This matching is to be made against the user's template; its calculations depend on the matching criteria [Jes05].

Chapter Three

Iris Recognition System Design

3.1 Introduction

In this chapter, the whole digital processing techniques involved in the designed system will be explained and discussed in some details. Generally, the designed system employed many digital processing methods. The adopted digital techniques have been turned into computer subroutines, these routines have been conducted in a broad programmable system, named ***Iris Recognition System "IRS"***.

3.2 Description of Iris Recognition System

IRS designed as two sub-systems: the Iris Enrollment System and the Iris Identification System. The input to the system is the iris image and the output is identified person or not. The system's design is shown in figure (3.1).

1. The Iris Enrollment System: this system is to enroll the iris in the database for further identification. The input to this module is the iris image. The first stage in this system performs the *preprocessing stage* that involves:

1. Image de-colorizing;
2. Edge detection using Marr-Hildreth method;
3. Eye-core-region detection using chain coding (contour following) process.

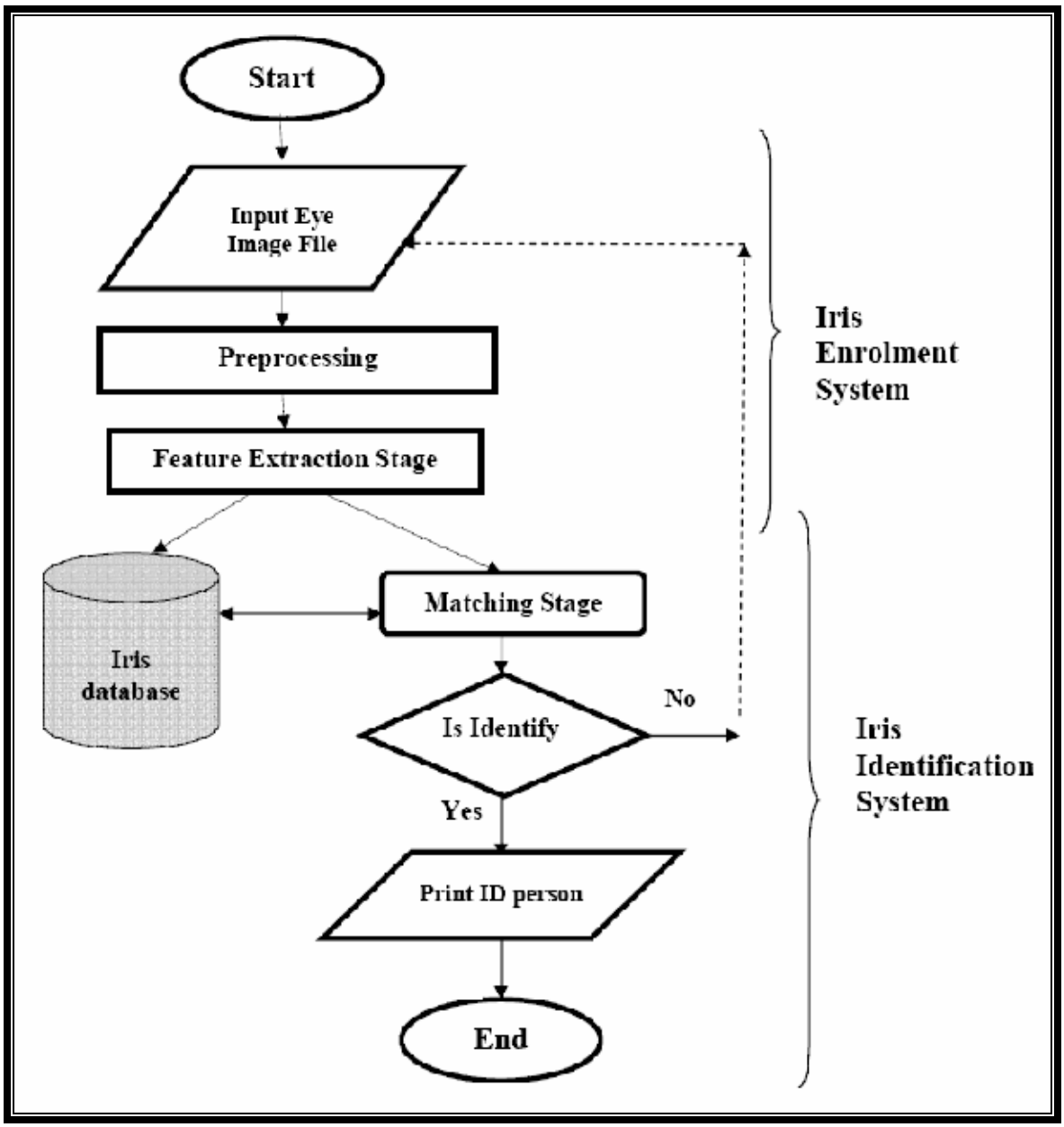

Figure (3.1) Iris Recognition System design

The second stage is *feature extraction stage* that involves:

1. Iris localization (extracting the correct iris region);
2. Perform Gabor filter;
3. Applying image normalizing process.

The result of this stage is creating feature vector for each input image that stored in a database.

2. The Iris Identification System: the input to this system is the feature vector. This system involves Classification process.

It is comprised matching stage, the feature of the input iris image, which is fed to this system, will be extracted, matching it with the stored iris images in the database to decides if it is in the database or not. The result of this system is Identified Person (ID) or not.

3.3 Design of Enrolment System

This system implies all the processing or steps required to determine the features vectors for an input image. The extracted features vectors in this system are stored in a database, to be utilized latter in the identification system. Figure (3.2) shows the implementation steps of the enrolment system.

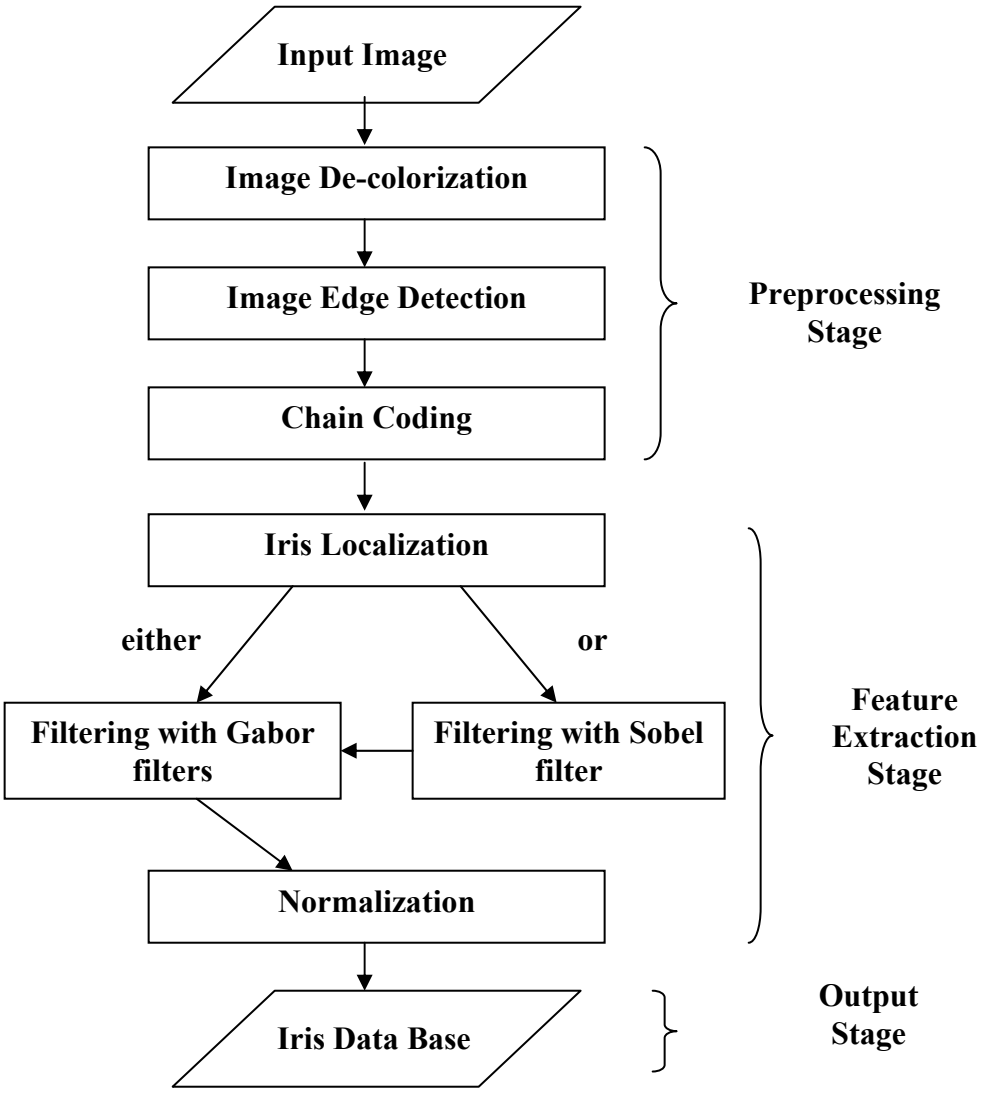

Figure (3.2) Implementation steps of the Enrolment system

3.3.1 Input Image File

The process of iris recognition is complex. It begins by scanning a person's iris. (i.e. the person stare into a camera for at least a second allowing the camera to scan his eye). The iris is captured in an image by infrared camera. The camera needs to be able to photograph a picture in the 700 to 900 nanometers range so that it will not be detected by the person's iris during imaging. The camera may or may not have a wide-angle lens yielding a higher resolution, but in either case a mirror is used to utilize feedback for the image. These conditions must be met

in order for the iris image to have the necessary 50-pixel minimum size of the iris radius [Jes05].

In this thesis, a standard (Joint Photographic Experts Group) JPEG image file of size 256×256 pixels and high resolution image can be used, by using an infrared camera. Figure (3.3) shown a type of infrared camera called **BMET330:**

Figure (3.3) BMET330

The BMET330 combines high precision, faster iris recognition and flexible system architecture for state-of-the art personal identification. These are another type of infrared cameras [Jes05]:

Figure (3.4) type of infrared cameras

3.3.2 Preprocessing Stage

Some preprocessing processes are used to make the data of the eye image more suitable for the primary data reduction and to make the analysis task easier. It is a necessary stage when the requirements are typically obvious and simple, such as ignoring all information that is not required for the application.

A. Image De-colorization

Converting the color image to grayscale = 256: basically each pixel in color image have three components of color (i.e. red, green, blue), the value of each color component is represented by one byte. The gray value to each pixel is computed by eq.(2.2). Applying this equation on all image pixels will lead to convert the color image to gray image as shown in figure (3.5). Algorithm (3.1) illustrates the implemented steps of reading JPEG file image and de-colorize the iris image into grayscale image.

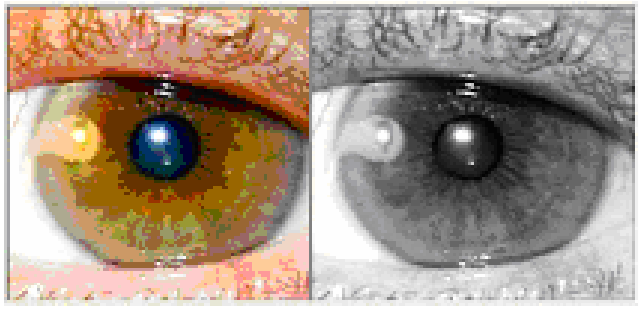

(a) colored image (b) grayscale image

Figure (3.5) Sample of an input eye-image

Algorithm (3.1) Input Image File & Image De-colorization

Input: Color image

Output: Gray Image *img(x,y)*

Begin

Open JPEG file images for read

Read JPEG file image

Put the JPEG file image in Pict1 and Pict2

Close file images

Set x, y as image width, height (size of the image = 256*256)

Initialize an array *img*(0 To y-1, 0 To x-1)

For all i ∈ [0 To y – 1] and j ∈ [0 To x – 1]

Set *img*(i, j) = grayscale value obtained from eq. (2.2)

$$Gray_{-image}(x,y) = \frac{\mathrm{Re}\,d_{-Band}(x,y) + Green_{-Band}(x,y) + Blue_{-Band}(x,y)}{3}$$

End loop j : End loop i

End.

B. Edge Detection process

In the edge detection process, the boundary is found, and the gray image is converted to a black and white image, this will make the determination of the eye's features become easy. In this work, Marr-Hildreth edge detection operator has been used. This technique has been suggested by David Marr and Ellen Hildreth in 1980 as being a model of human visual processing. As it has been mentioned before in eqs.(2.3), (2.4), (2.5), (2.6), and (2.7), (2.8), "*the only threshold value affected in this technique is* σ", edge images obtained with different σ are demonstrated in figure (3.4) where σ = (0.5, 3, and 12).

Therefore, to avoid the noise detection of small standard deviation (STD) when σ = 0.5 as shown in figure (3.6-a), and region merging of large standard deviation when σ = 12 as shown in figure (3.6-b), so, by try and error, a fixed standard deviation value σ =3 has been chosen as shown in figure (3.6-c), that called *Fixed Thresholding method*. Algorithm (3.2) illustrates the implemented steps of Marr-Hildreth edge detection.

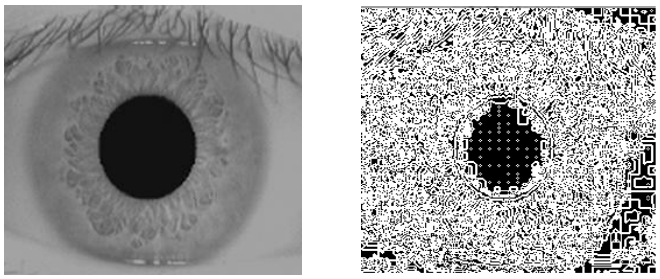

(a) Small σ = 0.5

(b) Large σ = 12

(c) Normal σ = 3

Figure (3.6) Marr-Hildreth edge detection with different σ values

Algorithm (3.2) Marr-Hildreth Edge Detection

Input: Gray Image *img(x,y)*

Output: Binary Image: EDG(x,y)

Begin

Initialize array *G*(0 To y-1, 0 To x-1)

Initialize array *Arr*(0 To y-1, 0 To x-1)

Initialize array *A*(0 To y-1, 0 To x-1)

Set STD = 3 "Gaussian Standard Deviation, Smoothing STD"

[*G*] = Gaussian function with given STD using eq. (2.3)

[*A*] = [G] $\otimes$ *img(x, y)*

∇^2 = Laplacian function

[*Arr*] = $\nabla^2 \otimes [G]$ Simulating Laplacian-Gaussian function using eq.(2.11)

$LoG(u,v) = \Im\{Arr(x,y)\}$ "Call FFT(*Arr(x,y)*) to Compute FFT of Laplacian-Guassian function . . . algorithm (3.3)"

$IMG(u,v) = \Im\{img(x,y)\}$ "Call FFT(*img(x,y)*) to Compute FFT of the eye-image . . . algorithm (3.3)"

$Limg(x,y) = \Im^{-1}\{LoG(u,v).IMG(u,v)\}$ "Compute 2nd order differentiation of eye-image, using IFFT $Limg(x,y) = \{\nabla^2 \otimes [A]\}$"

EDG(x,y) = Zer{*Limg(x,y)*} "Performing zero-crossing operation using eq.(2.8)"

End.

Algorithm (3.3) Fast Fourier Transform (FFT)

NOTE: the FFT is usually performed on 1D-function, for images the FFT runs on image-rows then image columns.

Input: 2D image array

Output: The inverse of the array

Begin

Let the image row or column array presented by *f(x)*, then

$$F(u) = \frac{1}{2}\{F_{even}(u) + F_{odd}(u)\}, \qquad \text{and}$$

$$F(u+M) = \frac{1}{2}\{F_{even}(u) - F_{odd}(u)W_{2M}^{u}\}$$

$$Where: M \text{ is the half - length of the function.}$$

$$W_{2M}^{u} = e^{-j(\frac{u}{2M})}$$

$$F_{even}(u) = \frac{1}{M}\sum_{x=0}^{M-1} f(2x)W_{M}^{ux}$$

$$F_{odd}(u) = \frac{1}{M}\sum_{x=0}^{M-1} f(2x+1)W_{M}^{ux}$$

The IFFT is the same as above but with an inverting sign $e^{+j(\frac{u}{2M})}$

Where: $j = \sqrt{-1}$

End.

C. Convolution

The convolution process will be used in this present work at two locations:

1. Performing edge detection by Marr-Hildreth method, the image needs to convolve with the Gaussian operator, and to perform LoG operator. See algorithm (3.2).
2. Performing Gabor filter, the simulated filter array (different orientation) with the image array. See algorithm (3.6).

D. Chain Coding

Marr-Hildreth edge image contains the boundary points of the iris (i.e. representing the bright points). Therefore, it is easy to follow them, using the (contour following) chain coding method. The transition from edge point to another can be presented by a directional indexing code (range between 1 to 8), which represent the 8-neighbors surrounding each edge image point. Chain coding technique facilitates the detection of the iris region.

The contour following process begin by finding the start point of the eye edge and checking the 8-neighbors of the start point to detect the next connected (chain) point. The coordinates of the start point is registered in the boundary array, after that start checking its neighbors in the clockwise manner, if one of them is an edge pixel (pixel value 255) then store this pixel in the boundary array and make it as a next test point and delete the old tested (start) point, then repeat this operation until finding out the new start point. In the case of finding out the correct start point then register the coordinates of the start point and all the connected adjacent points. Finally, if the starting edge-point is detected again at the search end and the result of the applied search method is circular, then find

the contour center $(\bar{x}, \bar{y})$ and average radius. Algorithm (3.4) illustrates the implemented steps of chain coding operation.

Algorithm (3.4): Eye's Core Detection using Chain Coding Method

Input: Edged Image EDG(x,y)

Output: Pupil-Core $(\bar{x}, \bar{y})$, Pupil-Radius $R_{Average}$

Begin

Search EDG(x,y) for edge-point, if found, then

Check around the edge-point for another edge (in clockwise direction)

If found, then move to the new edge-point:

Continue till no further edge is existed

If the starting edge-point is detected again at the search end then

Its close contour "close contour condition"

End if

If it is closed contour then

Find the contour center $(\bar{x}, \bar{y})$, using average of x and y coordinates of the searched points; i.e.

$$\bar{x} = \frac{\sum_{I=1}^{end\ of\ contour} x_I}{\text{Number of contour points}}, \quad \bar{y} = \frac{\sum_{I=1}^{end\ of\ contour} y_I}{\text{Number of contour points}}$$

Find contour average radius: $R_{Average} = \frac{\sum_{i=1}^{end\ of\ contour} \sqrt{(x_i - \bar{x})^2 + (y_i - \bar{y})^2}}{\text{Number of contour points}}$

To be continue

Find standard deviation of detected edge points:

$$Strd = \frac{\sum_{i=1}^{end\ of\ countor} [(\sqrt{(x_i - \bar{x})^2 + (y_i - \bar{y})^2}) - R_{average}]^2}{\text{Number of contour points}}$$

End if

End if

The contour represents Iris region,

If *Strd* <= 4 and $R_{Aaverage}$ >= 15 and $R_{Aaverage}$ <= 55 then

Draw a circle around the center, pupil and iris

Else Test Failed

End if

Call algorithm (3.5) "Extracting region of interest surrounding the eye's pupil point"

End.

3.3.3 Feature Extraction Stage

The main steps in the feature extraction algorithm are:

1. Iris Localization (extract the correct region of interest) for the iris image;
2. Filtering the region of interest in eight different directions using a bank of Gabor filters (eight directions are required to completely capture the local ridge characteristics in an iris image while only four directions are required to capture the global configuration); or using both Sobel and Gabor filters.
3. Perform iris normalization on the filtered images to remove the effects of noise.

A. Iris Localization

Once the chain coding operation performed, and the core point of the iris was located. There are two variables within the image that are needed to fully locate the iris: the core-point coordinates $(\bar{x}, \bar{y})$, and the pupil radius $R_{Average}$. The iris is localized in two steps:

1. The iris is an annular portion between the pupil (inner boundary) and the sclera (outer boundary). Both the inner boundary and the outer boundary of a typical iris can approximately be taken as circles. However, the two circles are usually not concentric as shown in figure (3.7). The exact parameters of these two circles are obtained by using chain coding operation, the first circle represent the distance between the center and the boundary of the pupil, which *Strd* <= 4, the second circle represent the iris region, which $R_{average}$ >= 15, and the boundary of the eye $R_{average}$ <= 55. See algorithm (3.4).

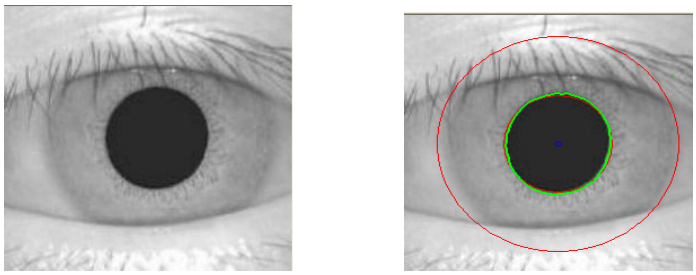

Figure (3.7) Iris center detection

2. Extract the region of iris in an image can be found by projecting iris image in horizontal and vertical direction, by computing the radius in a certain region determined in the first step using eq.(2.13).

Figure (3.8-b) illustrates the extracting region of interest surrounding the eye's pupil point. Algorithms (3.5) illustrate the implemented steps of extracting region of interest surrounding the eye's pupil point.

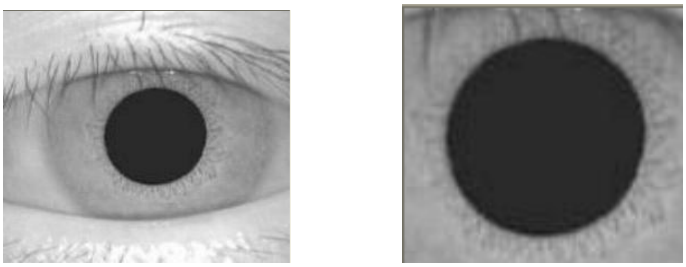

(a) **(b)**

Figure (3.8) Extracting region of interest surrounding the eye's pupil point
(a) Original image of size (256×256)
(b) Extract iris region of size (128×128)

Algorithm (3.5): Extracting Region of Interest surrounding the Eye's pupil point

Input: *img(x,y)*, Pupil-Core ($\bar{x}, \bar{y}$), $R_{average}$

Output: Extracted iris image *Eimg(x,y)*

Begin

Initialize an array *Eimg*(1 To 128, 1 To 128)

Extract *img(x, y)* of size (256×256) into *Eimg*(x, y) of size (128×128) around $\bar{x}, \bar{y}$ and $R_{average}$

End.

B. Sobel Filter

Digitally, differential operator may be presented by either 2×2 or 3×3 windows. In this work, the extracted image array *Eimg(x, y)* is specially processed by Sobel operator before filtering it with Gabor filters only for matching purposes. Figure (3.9) demonstrates Sobel edge detection process, the following template (window) represents 3×3 Sobel operator:

$$\begin{matrix} 1 & 2 & 1 \\ 0 & 0 & 0 \\ -1 & -2 & -1 \end{matrix} \qquad \begin{matrix} 1 & 0 & -1 \\ 2 & 0 & -2 \\ 1 & 0 & -1 \end{matrix}$$

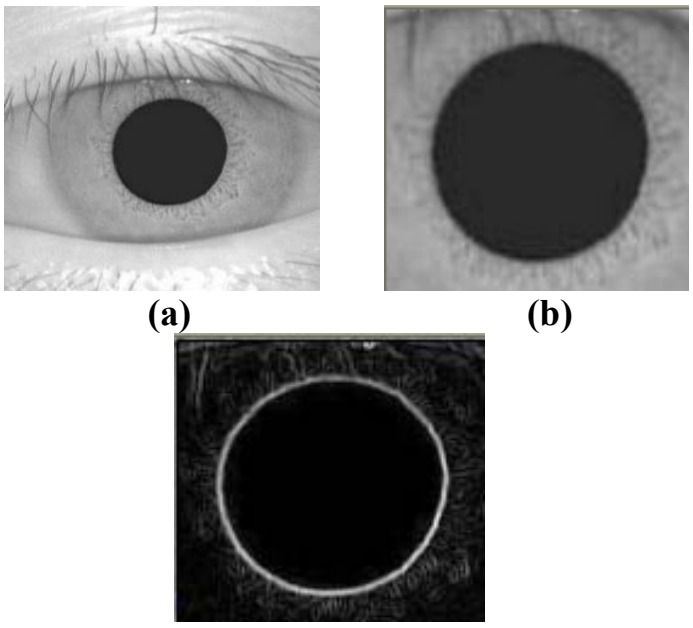

(a) **(b)**

(c)

Figure (3.9) Illustrating Sobel edge detection process
(a) Original grayscale image (256×256) (b) Extracted iris image (128×128)
(c) Edge image with Sobel filter (128×128)

C. Gabor Filters

As it's mentioned before in chapter two in eq.(2.21), the convolution with Gabor filters is still the major contributor to the overall feature extraction time. The filter frequency f is used to the average ridge frequency (1/k), where k is the average inter-ridge distance. The average inter-ridge distance is approximately 6 pixels in a 300 dpi iris image.

If f is too large, spurious ridges are created in the filtered image whereas if f is too small, nearby ridges are merged into one. Eight different values for θ (0°, 22.5°, 45°, 67.5°, 90°, 112.5°, 135°, and 157.5°) where used with respect to the x-axis.

The extracted region of interest in an iris image is convolved with each of these eight filters to produce a set of eight filtered images. These eight directional-sensitive filters capture most of the global ridge directionality information as well as the local ridge characteristics present in the iris.

Illustrate this through reconstructing an iris image by adding together all the eight filtered images. The reconstructed image is very similar to the original image and slightly blurred (degraded) due to lack of orthogonality among the filters as shown in figure (3.10).

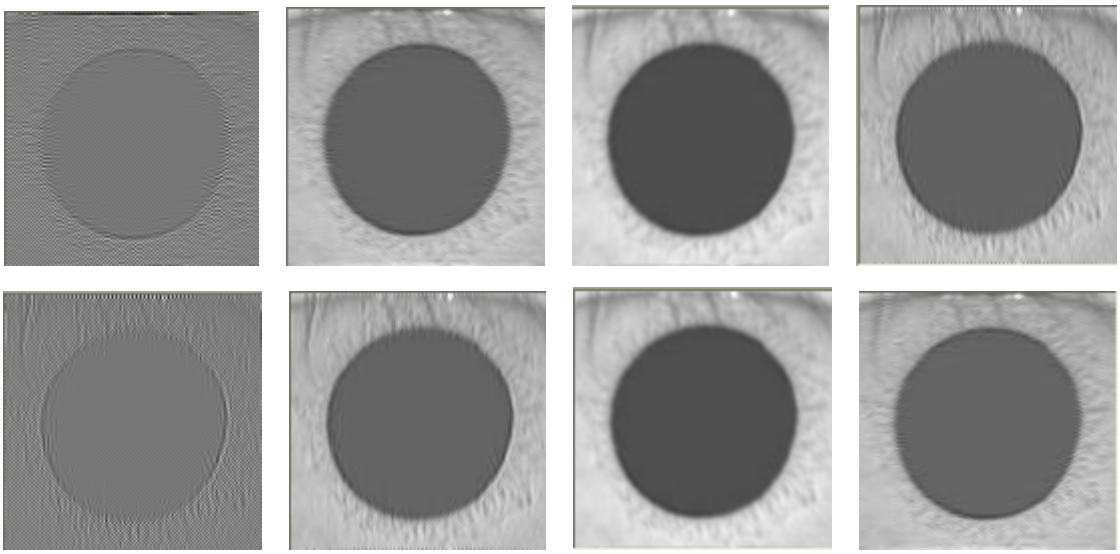

Figure (3.10) Demonstration of eight Gabor filtered images of size (128×128)

if $\delta_{x'}$ and $\delta_{y'}$ (standard deviations of the Gaussian envelope) values are too large, the filter is more robust to noise, but is more likely to smooth the image to the extent that the ridge and valley details in the iris will be lost. However, If $\delta_{x'}$ and $\delta_{y'}$ values were too small, the filter will not be effective in removing the noise. After trying and error found the suitable values of $\delta_{x'}$, $\delta_{y'}$ = 0.65, see figure (3.11). Algorithm (3.6) illustrates the implemented steps of Gabor filters.

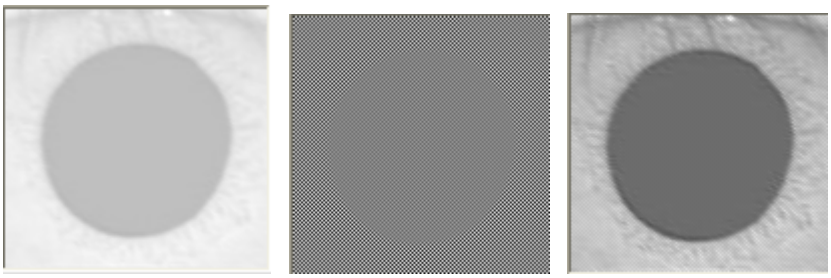

(a) **(b)** **(c)**

Figure (3.11) Examples of implementing different standard deviations of the Gaussian values (a) value too large = 6 (b) value too small = 0.005 (c) Normal = 0.65

Algorithm (3.6) Gabor filter

Input: Extracted iris image *Eimg(x, y)*, Pupil-Core ($\bar{x}, \bar{y}$)

Output: Eight different images by 8 different angles θ

Begin

Set $\delta_{x'}$, $\delta_{y'}$ = 0.65 "as standard deviation of Gaussian function"

Initialize array *Gab*(1 To 128, 1 To 128)

Initialize array *GE*(1 To 128, 1 To 128)

$IMG(u,v) = \Im\{Eimg(x,y)\}$ "Call FFT(*Eimg*(*x,y*)) to compute FFT of the eye-image ……algorithm(3.3)"

Convert θ from degree to radiant form

Where θ (0°,22.5°,45°,67.5°, 90°,112.5°,135°,157.5°)

[*Gab*] = Gabor function with given Stds and θ using eq.(2.21)

$[GE] = [Gab] \otimes [Eimg]$ "Compute the convolution of edged image with Gabor function"

$Gab(u,v) = \Im\{[GE]\}$ "Call FFT(*GE*(*x,y*)) to compute FFT of Gabor filters function ……algorithm(3.3)"

$Gimg(x,y) = \Im^{-1}\{Gab(u,v)\}$ "Call IFFT(*Gab*(*u,v*)) …… algorithm(3.3)"

Display the *Gimg*(*x,y*) as 8 different images by 8 different angles

End.

D. Iris Normalization

The size of the same iris taken at different times may be variable in the image as a result of changes in the camera-to-face distance. Due to stimulation by light or for other reasons the pupil may be constricted or dilated. These factors will change the iris resolution, and the actual distance between the pupillary and the limbic boundary.

To solve these problems, the iris image is processed to ensure the accurate location of the virtual circle and to fix the resolution, by normalize the region of interest of *Gimg(x, y)* to a constant mean M_0 and variance V_0.

Normalization is performed to remove the effects of sensor noise and gray level deformation and reduce the variations in gray level values along ridges and furrows, Samples of normalized the filtered images are shown in figure (3.12).

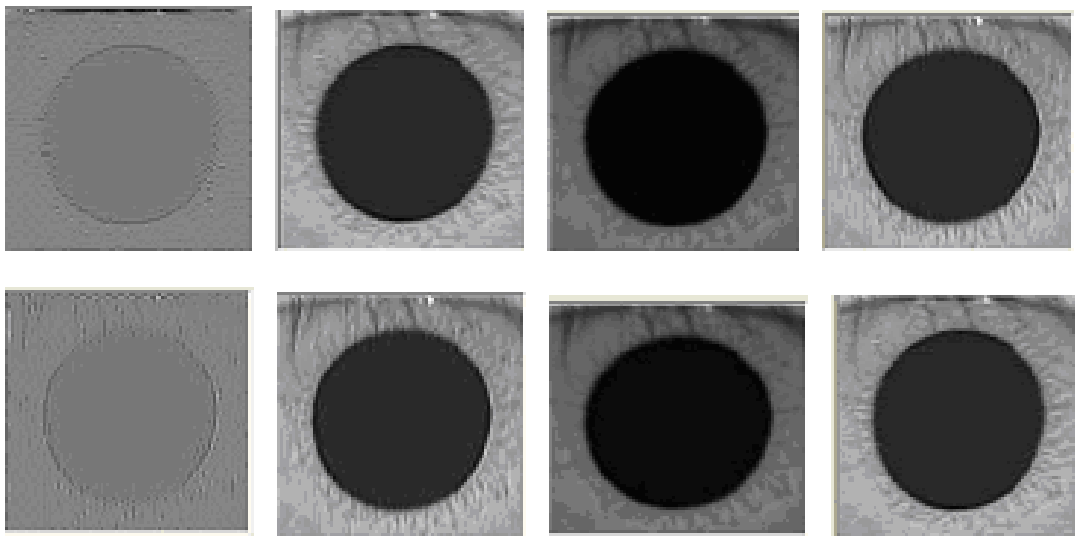

Figure (3.12) Demonstration of the normalized images of size (128×128)

Figure (3.13-a) shows an example of this normalization scheme. When M_0 and V_0 set to 200, the details (ridge and valley) of this image are lost for this experiment. The values of both M_0 and V_0 are set to 20, see figure (3.13-b). In this values normalization is not effective to a clearness, so that the suitable values

of M_0 = 20 and V_0 = 50, see figure (3.13-c). Algorithm (3.7) illustrates the implemented steps of iris normalization.

(a) **(b)** **(c)**

Figure (3.13) Normalized the region of interest a round core point when (a) set the values of both M_0 and V_0 to 200 (b) set the values of both M_0 and V_0 to 20 (c) set the values of M_0 to 20 and V_0 to 50

Algorithm (3.7) Normalization

Input: *Gimg*(x, y)

Output: Normalized images *N(x, y)*

Begin

Set $M_0 = 20$: Set $V_0 = 50$ "proposed mean and variance values"

Set $M_i = 0$: Set $V_i = 0$

$M_i = M_i$ + mean of each value of G*img(x, y)*

$V_i = V_i + (\text{variance} - M_i)^2$

If *Gimg(x, y)* >= M_i then

$$N(x, y) = M_0 + \sqrt{\frac{V_0 \times (img(x,y) - M_i)^2}{V_i}},$$

Else $$N(x, y) = M_0 - \sqrt{\frac{V_0 \times (img(x,y) - M_i)^2}{V_i}},$$

Display the 8 normalized images *N(x, y)*

End.

3.3.4 Output Stage

The result of this stage is creating feature vector for each input image that stored in a database or matched with the database, by tessellate the region of interest around core point.

The globalized iris region is sliced into five circular strips or sectors S_i around the core point $(\bar{x}, \bar{y})$, where the i^{th} sector S_i is computed in terms of parameters (r, θ), based on transforming the Cartesian presentation (*x, y*) into the polar (r, θ) form.

A total of 40 features are extracted for each iris extracted image; eight globalized images, and five for the sliced sectors as shown in figure (3.14).

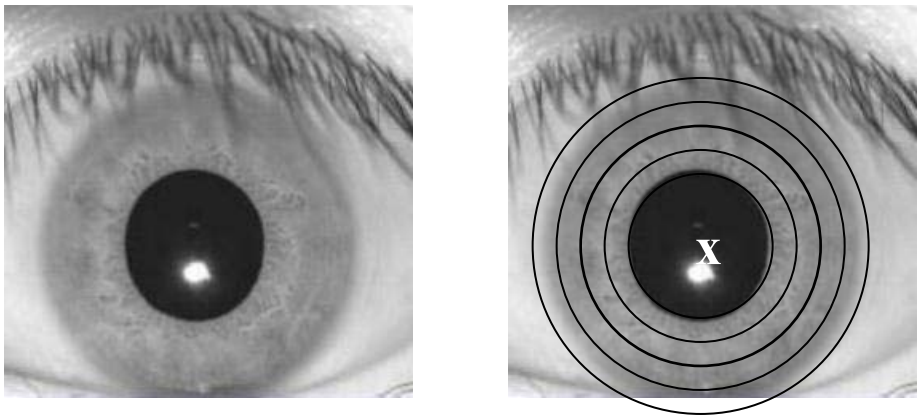

Figure (3.14) Core-point (x), the region of interest, and 5 sectors superimposed on an iris

A. Feature Vector

Let $N_{i\theta}$ *(x,y)* be the normalized filtered image for sector S_i around θ-direction.

Now, $\forall \; i \in \{0,1,...., 39\}$ and $\theta \in \{0^\circ, 22.5^\circ, 45^\circ, 67.5^\circ, 90^\circ, 112.5^\circ, 135^\circ, 157.5^\circ\}$, the feature value, $Vec_{i\theta}$, is the Average Absolute Deviation (AAD) from the mean defined as:

$$\text{Vec}_{i\theta} = \frac{1}{n_i}\left(\sum |N_{i\theta}(x,y) - Mean_{i\theta}|\right) \quad (3.1)$$

Where n_i is the number of pixels in S_i and $Mean_{i\theta}$ is the mean of pixel values in $N_{i\theta}(x,y)$ in sector S_i. The AAD of each sector in each of the eight filtered images defines the components of the feature vector.

The 40-dimensional feature vectors (IrisCodes) for eye images are listed in table (4.4) in chapter four. Algorithm (3.8) illustrates the implemented steps of create the feature vector.

Algorithm (3.8) Create the feature vector

Input: $R_{average}$, $N(x, y)$: the normalized filtered image

Output: Circular Strip Width: CSW, Last radius: $LR_{average}$,
Feature Vector: Vec(40)

Begin

Set $S = 5$ "number of sectors"

Initialize array Vec(1 To 40)

Compute CSW = Int((64 - $R_{average}$)/ 5) "the width of each sector"

Compute $LR_{average} = R_{average}$ + CSW * 5

If $LR_{average} > 64$ Then $LR_{average} = 64$

Set Vec(i) = 0 for all i ∈ [1 To 40] as a feature vector array

Convert Cartesian presentation (x, y) into the polar (r, θ) form

Compute mean of pixel values in $N_{i\theta}(x,y)$ in sector S_i

Compute the Vec(i) for the input image using eq.(3.1)

Ether Call Add to database . . . algorithm (3.9)

Or Call Matching with database . . . algorithm (3.10)

End.

B. Iris Data Base

In this thesis, iris database contains imagery for a total of 10 different irises. All of these 10 irises enrolled then stored in the Iris Database.

Algorithm (3.9) Add to database

Input: A new person

Output: Stored the new person in infoperson-file

Begin

Open infoperson-file to insert

Enter the file number

Full the fields with data and eye image

Store the information in the infoperson-file

Close infoperson-file

End.

3.4 Design of Identification System

The identification system consists of the stages that shown in figure (3.15). The preprocessing stage and feature extraction stages that their steps are described before in the *iris enrollment system* will be used in *iris identification system*, too with few differences. Figure (3.15) illustrates the different processes and stages in their sequences that are implemented in iris identification system.

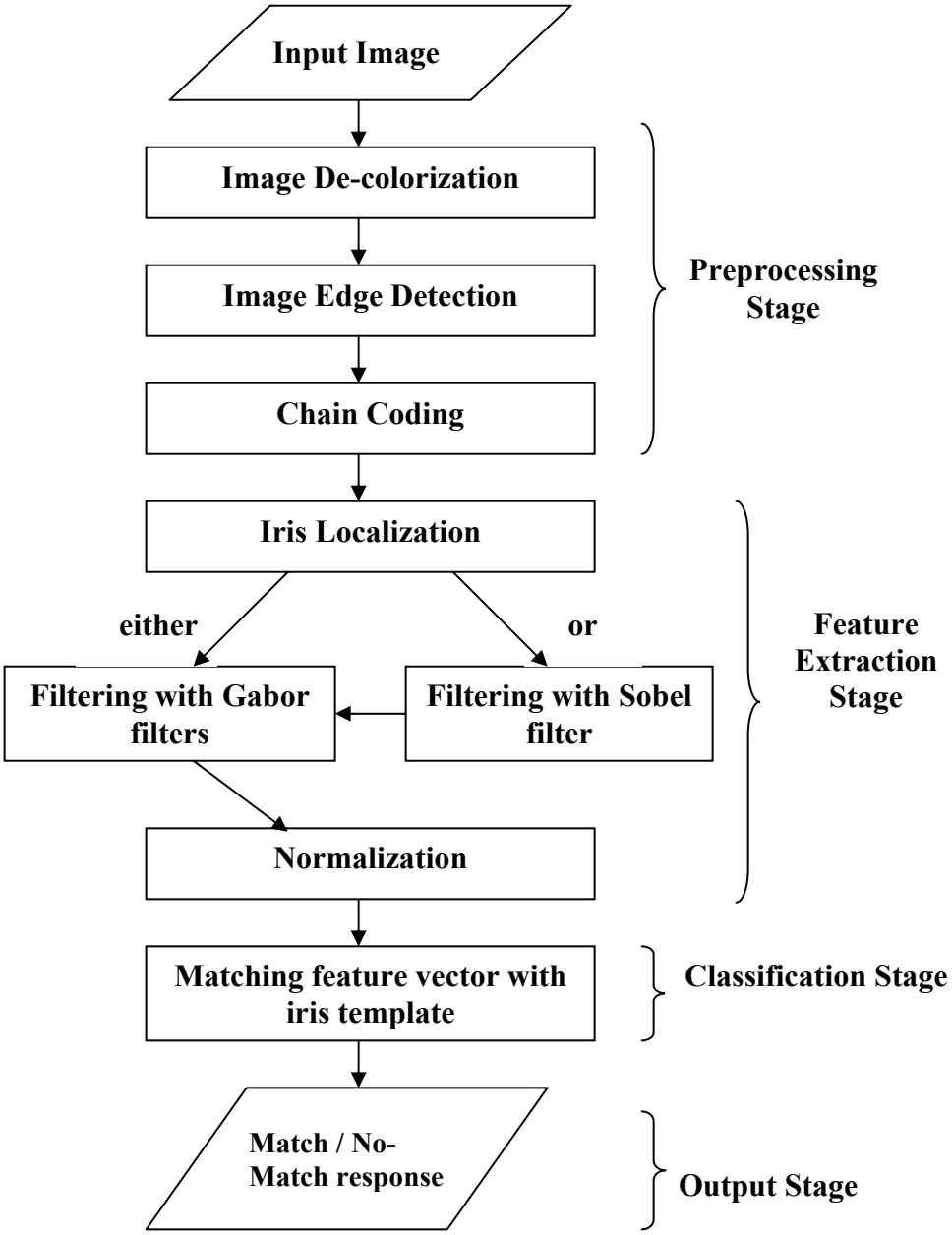

Figure (3.15) Implementation steps of the Identification system

Note that, the input, preprocessing, and feature extraction stages of *identification system* are similar to those of *enrollment system* in their implemented steps with simple difference. Since their discussion and algorithms have been described before, thus it is not necessary to present them again in this system. Only the two other steps (classification and output stages), and the only

simple difference which is appended to the feature extraction stage for matching process will be discussed in the following sections.

3.4.1 Classification Stage

Iris matching is based on finding the minimum distance between the corresponding IrisCodes. After performing Gabor filters and a feature vector created, the image is divided into 5 sectors by different 8 angles, where $\theta \in \{0^\circ, 22.5^\circ, 45^\circ, 67.5^\circ, 90^\circ, 112.5^\circ, 135^\circ, 157.5^\circ\}$. For each person, there are 40 features stored in the database.

In this thesis, minimum distance is adopted and used to test the similarity between the preserved featured vectors with any newly input one; i.e. if $V_{Pre}(i)$ represents the preserved feature's vector and, $V_{New}(i)$ the newly input feature's vector, then the *Minimum-Distance-Classifier (MDC)* is given by;

$$MDC = \sqrt{\sum_{i=1}^{n} (V_{\_Pre}(i) - V_{\_New}(i))^2} \tag{3.2}$$

Where, n represents the number of adopted test features.

In this present thesis, the tested features are consider similar (i.e. belongs to the same person), if *MDF* <= 4, where *MDF* is minimum value of *MDC*. Algorithm (3.10) illustrates the implemented steps of matching stage.

Algorithm (3.10) Matching with database

Input: Feature Vector: Vec(40)

Output: Defined or Undefined Person

Begin

MDF = 4

Open Database-file for read "file of the feature vector"

Read the Vec(i) for all i ∈ [1 To 40]

While not EOF

MDC = Compute the Minimum-Distance between $V_{Pre}(i)$ and $V_{New}(i)$ for the input person using eq.(3.2)

Close the Database-file

If *MDC* = 0 or *MDC* < = *MDF* then

The person is identified

Open infoperson-file for read

Read the file

Display the information of each person from the file

Close the infoperson-file

Else

Undefined Person

End If

End.

3.4.2 Output Stage

This stage is responsible for displaying the person's name and other information with his personal image (if he exists). However, when no match occurred, then a message will be displayed to notify the user that no matched image was found and the person's claimed identity was denied (i.e. undefined person).

Chapter Four

Experimental Results and Discussion

4.1 Introduction

As it has been mentioned in chapter three, the ***IRS*** designed as two sub-systems: i.e. the *Iris Enrollment System* and the *Iris Identification System*. The result of the enrollment system creates feature vector for unknown persons. While the identification system extracts feature vector of the unknown person and performs matching with the features vectors stored in the database that are belong to the 10 persons, each one has 3 samples of eye images, one of them stored in the database and the two others used for matching purposes, (i.e., image0 is the original image that stored in the database, image1 is the noised image with Gaussian of $\alpha = 1.25$ and variance = 100, and image2 is the rotated image with $\beta = 1$. Figure (4.1) shows samples of eyes. The eyes images are JPEG and the size of each test image is 256×256 pixels. The matching process will be performed by utilizing the Minimum Distances method.

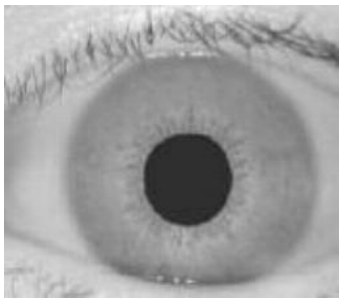

(Image1)

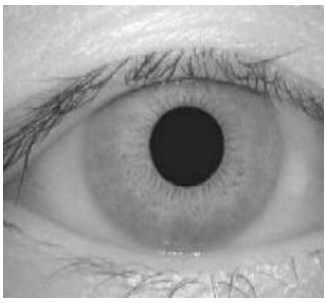

(Image2)

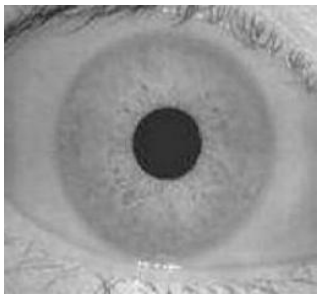

(Image3)

(Image4)

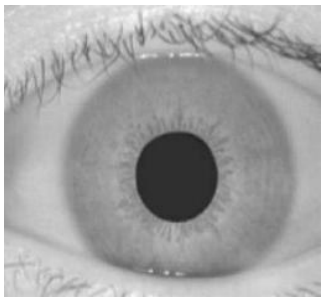

(Image5)

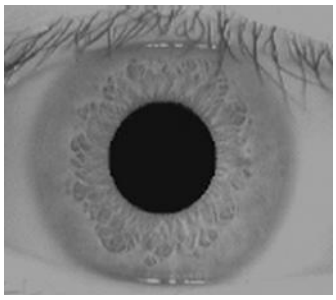

(Image6)

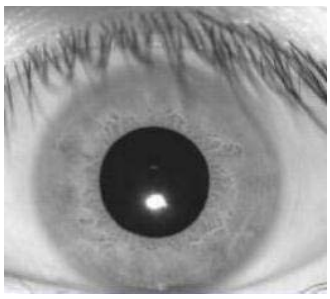

(Image7)

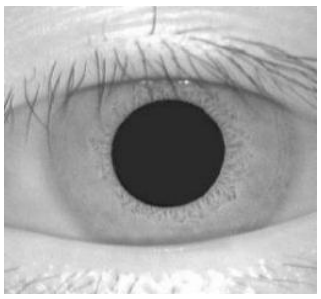

(Image8)

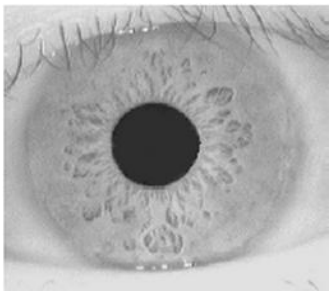

(Image9)

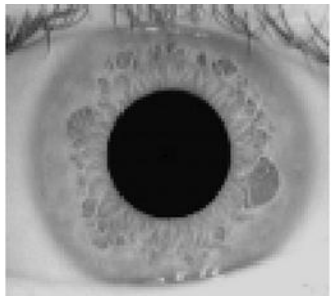

(Image10)

Figure (4.1) Examples of some eyes

Some of images have been skipped from Database because of the following reasons:

1. The core point was not located at the image's center, and therefore an appropriate region of interest could not be established and,
2. The quality of the image was poor because of blinking, out-of-focus, motion blur, out of line-of-sight as shown in figure (4.2).

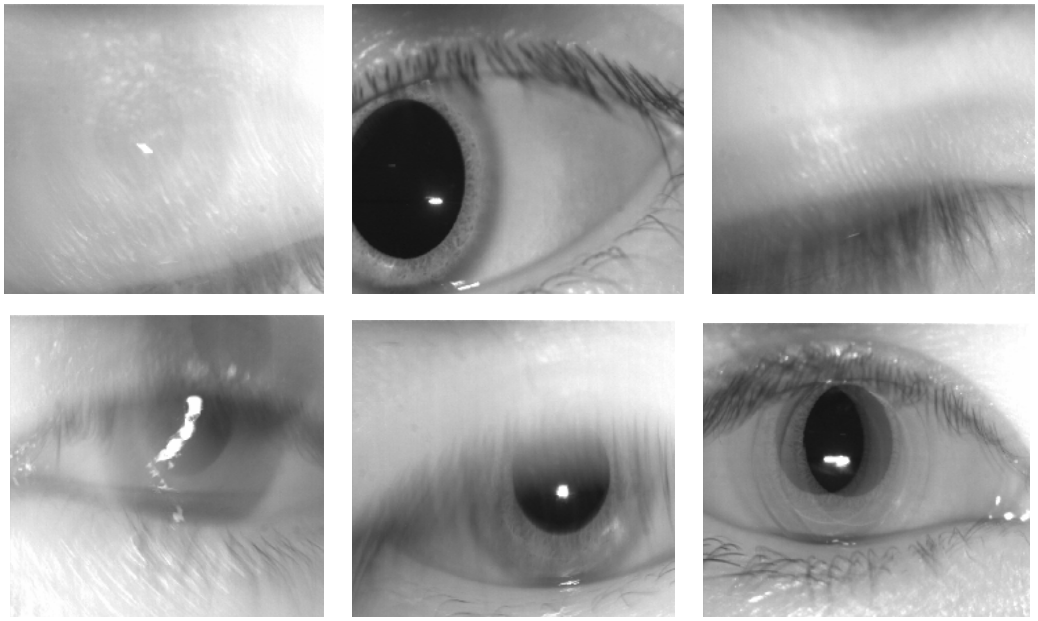

Figure (4.2) Samples of rejected images

In the biometric system operations; the identification mode, there are two possible outcomes; i.e. *Successful Test* or *Failer Test*.

The verification accuracy of the iris representation and matching approach is laid in its matching results between the input iris image with those priority featured iris images preserved in the database. A matching is labeled *Identified Person* if the same iris did yield identical IrisCode, see table (4.1).

Table (4.1) Examples of genuine acceptance (minimum distance is 0) using Sobel with Gabor filters and Gabor filter alone										
No	**Name**	**x, y coordinates of core point when Stored Iris**		**x, y coordinates of core point when matched with the database**		**Pupil Radius**	**Last Radius**	**Circler strip width**	**MDT**	**Matched Result**
		$\bar{x}$	$\bar{y}$	$\bar{x}$	$\bar{y}$					
1	Image1	141	152	141	152	38	63	5	0	**Success**
2	Image2	147	124	147	124	33	63	6	0	**Success**
3	Image3	134	123	134	123	31	61	6	0	**Success**
4	Image4	133	127	133	127	31	61	6	0	**Success**
5	Image5	140	151	140	151	37	62	5	0	**Success**
6	Image6	130	132	130	132	53	63	2	0	**Success**
7	Image7	120	157	120	157	47	62	3	0	**Success**
8	Image8	135	131	135	131	48	63	3	0	**Success**
9	Image9	120	127	120	127	36	61	5	0	**Success**
10	Image10	124	135	124	135	46	61	3	0	**Success**

Also for noised and rotated images a matching is labeled *Identified Person* when IrisCode for input eye nearly same any eye in database or the core point location of input eye nearby the core point location of stored eye in Database (i.e. minimum distance <= threshold (*MDF* = 4)). A matching is labeled *Undefined Person* if the eye did not yield nearly minimum distance (i.e. minimum distance > threshold (*MDF* = 4)), see table (4.2) and table (4.3). Figure (4.3) and (4.4) illustrates the charts of the comparison of the noised and rotated images with the database.

Table (4.2) Examples of matching the noised images with the database using Gabor filter alone

Noised Images	Database images									
	Image 1	Image 2	Image 3	Image 4	Image 5	Image 6	Image 7	Image 8	Image 9	Image 10
Image1	89	311	207	169	112	293	378	362	228	514
Image2	320	57	289	199	329	311	234	124	116	492
Image3	276	179	137	173	285	333	320	140	148	542
Image4	233	164	186	100	240	330	291	165	179	523
Image5	138	215	209	143	137	285	288	266	139	508
Image6	321	250	402	302	300	100	315	281	237	311
Image7	375	136	386	290	376	290	65	181	217	449
Image8	400	137	305	267	407	337	240	36	178	450
Image9	270	117	243	153	277	285	266	130	88	474
Image10	461	342	524	426	438	186	391	345	327	175

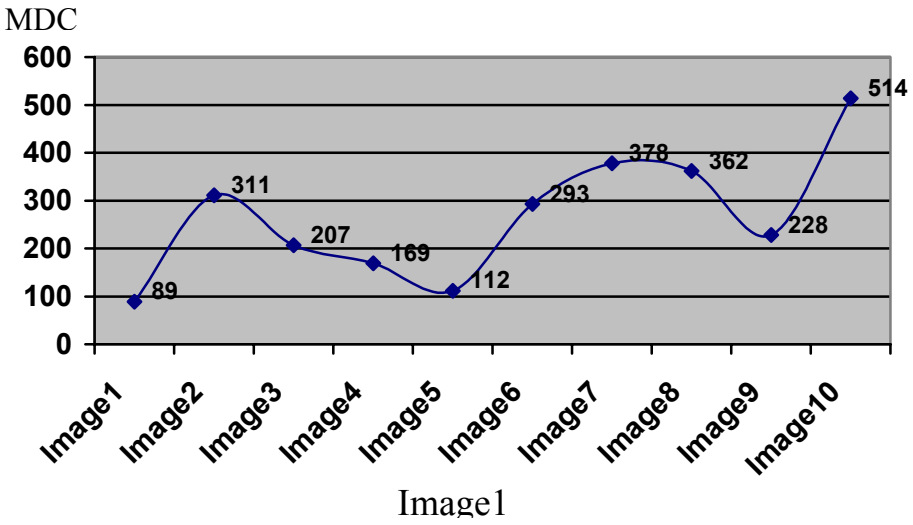

Image1

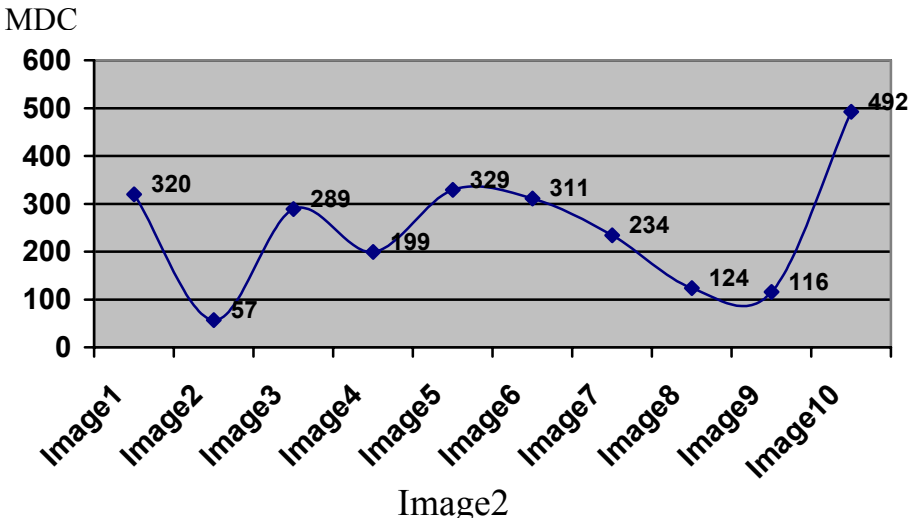

Image2

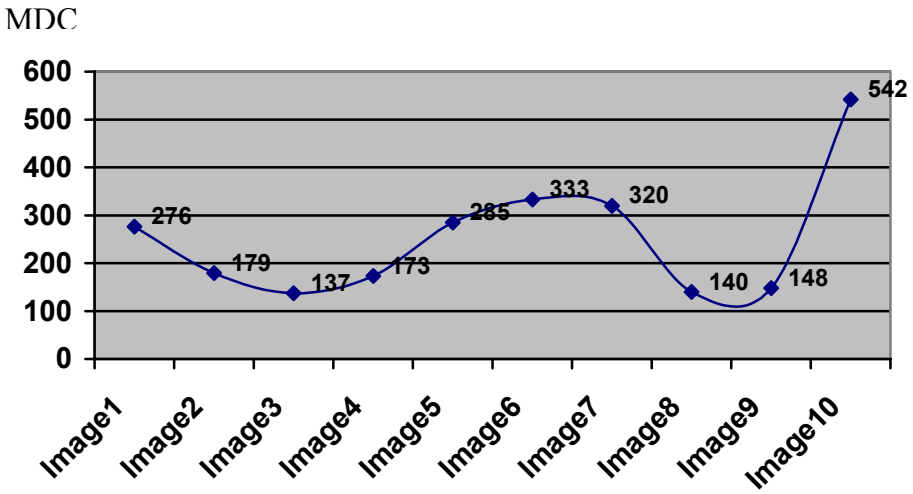

Image3

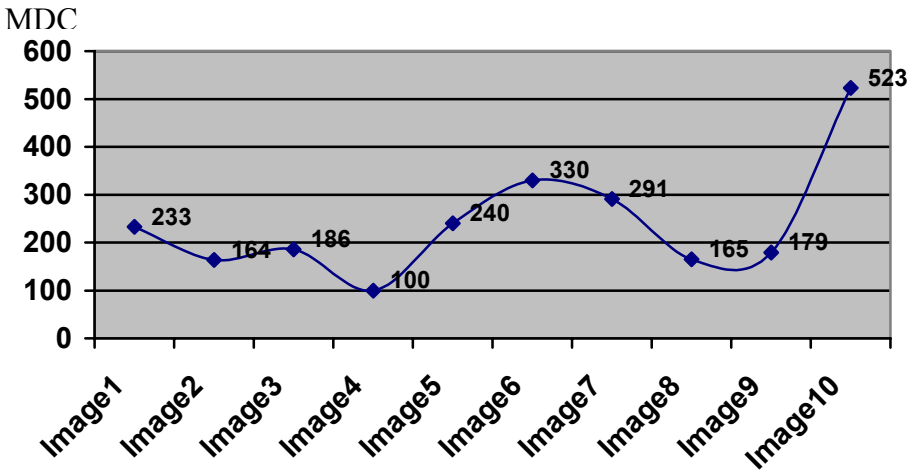

Image4

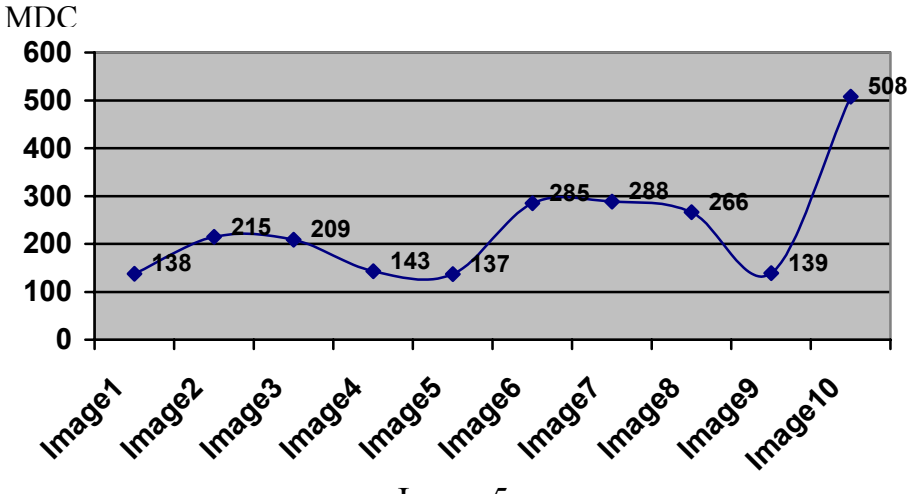

Image5

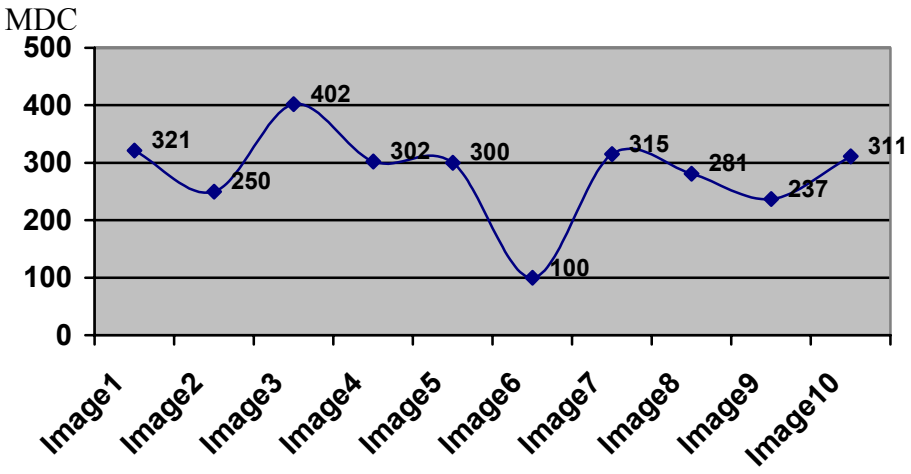

Image6

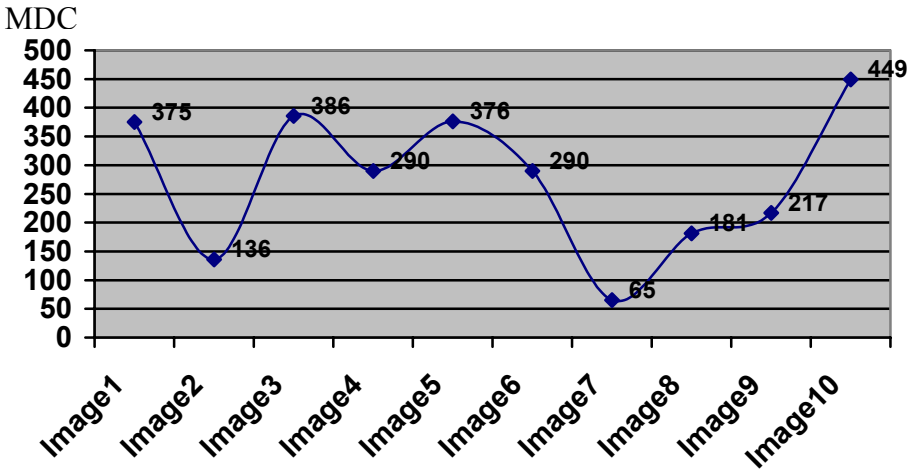

Image7

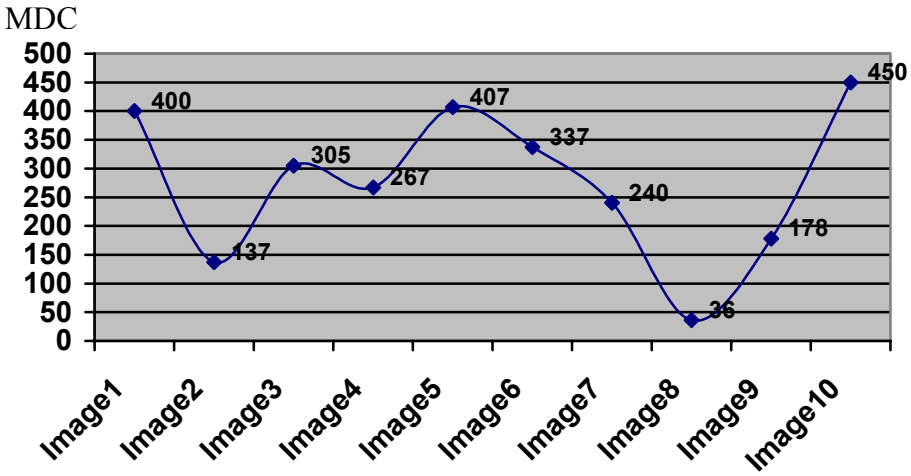

Image8

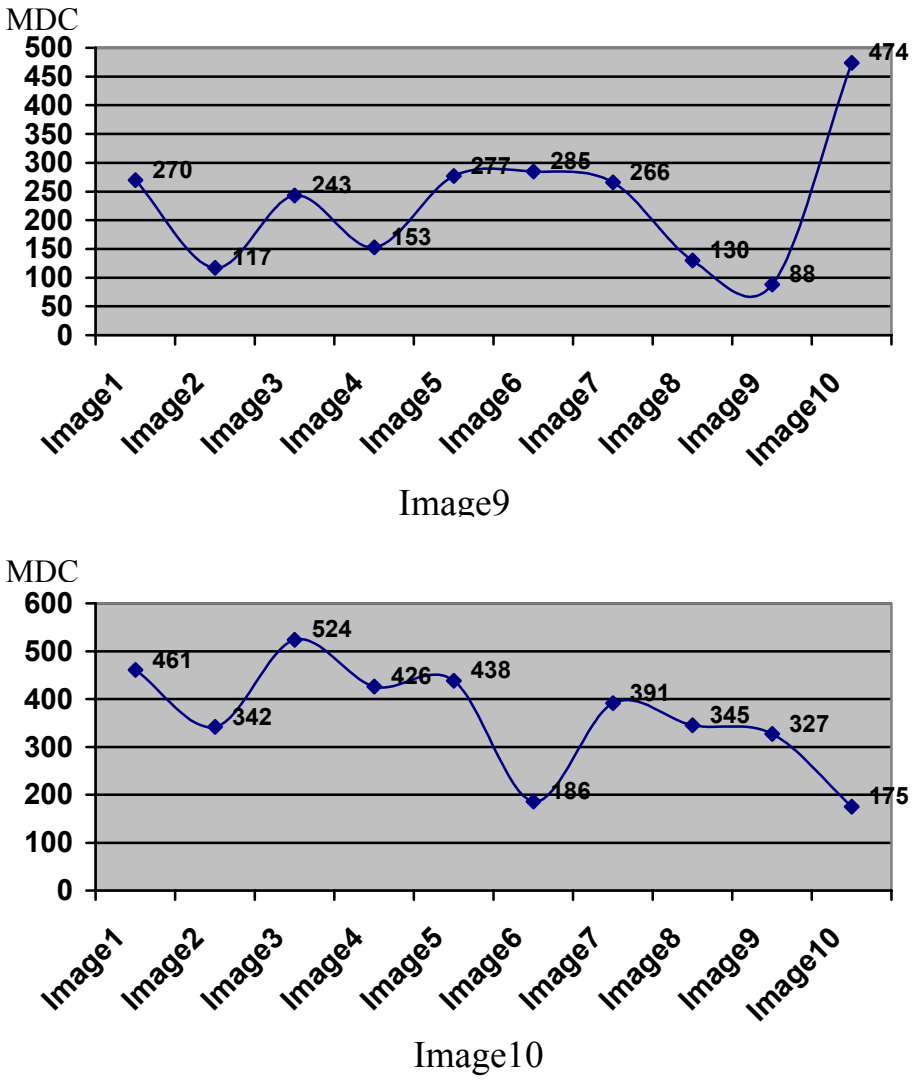

Figure (4.3) Illustrates the comparison of the noised images with the database using Gabor filter alone

Table (4.3) Examples of matching the rotated images with the database using Gabor filter alone

Noised Images	Database images									
	Image 1	Image 2	Image 3	Image 4	Image 5	Image 6	Image 7	Image 8	Image 9	Image 10
Image1	20	349	159	169	27	401	426	404	254	626
Image2	345	26	340	246	356	298	185	115	147	471
Image3	176	299	39	155	183	453	432	270	196	666
Image4	123	288	98	62	134	443	415	299	189	657
Image5	64	323	179	155	43	337	388	378	228	564
Image6	456	329	531	435	435	97	340	354	334	206
Image7	399	182	450	354	400	292	45	223	269	413
Image8	346	175	357	261	353	279	272	156	206	410
Image9	220	159	217	181	225	331	286	186	28	510
Image10	594	451	653	561	571	213	446	432	456	52

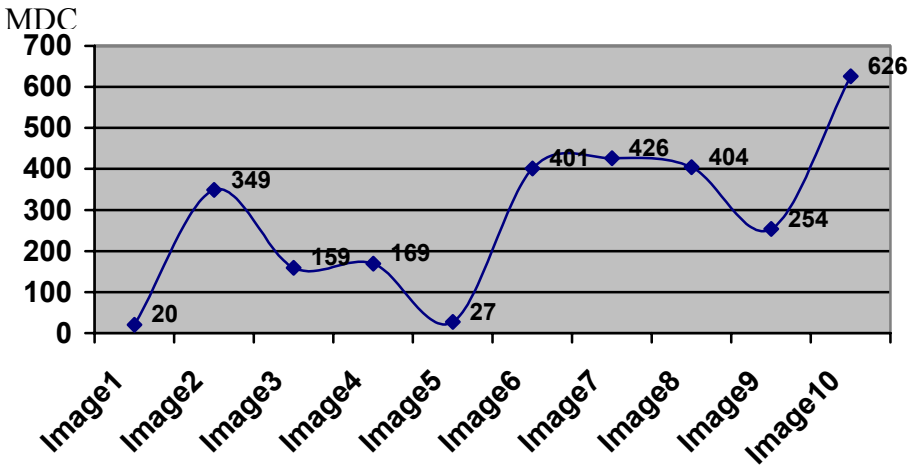

Image1

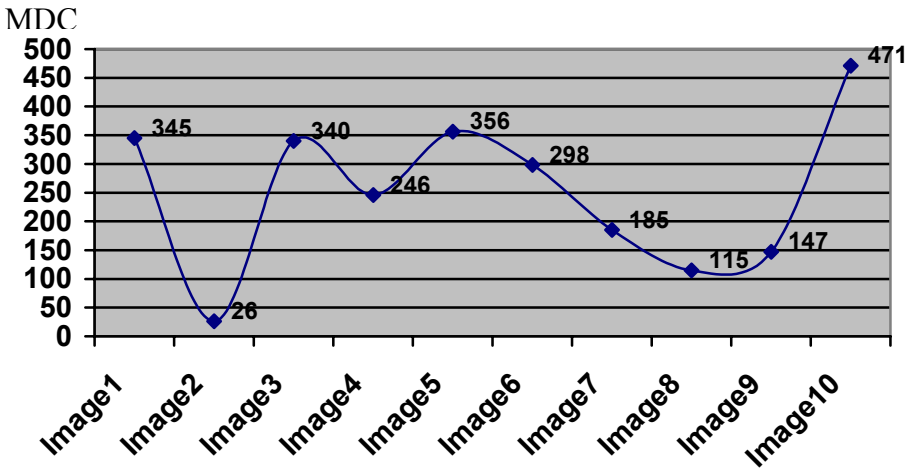

Image2

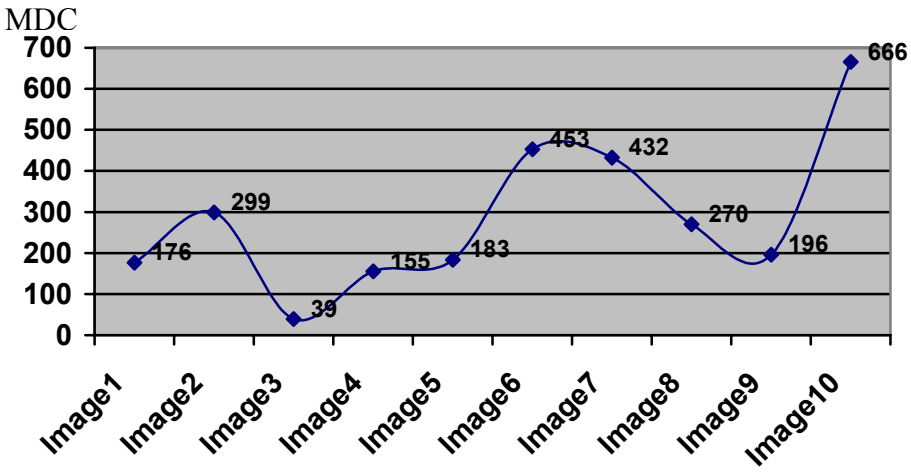

Image3

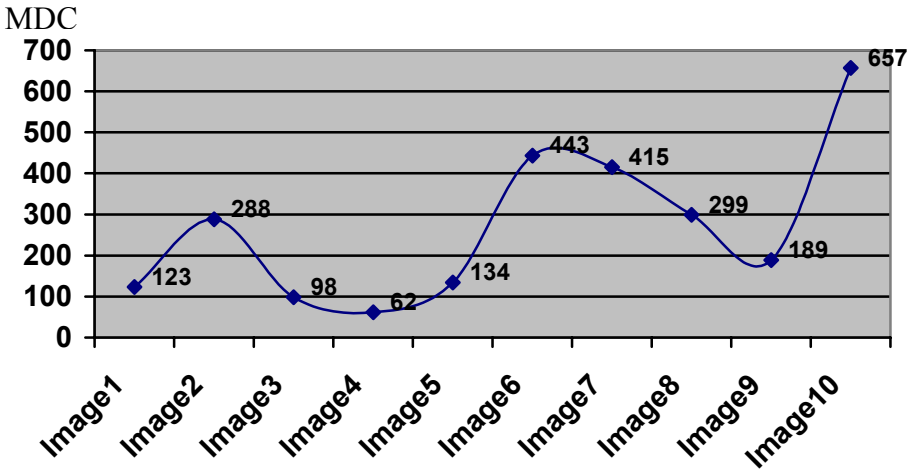

Image4

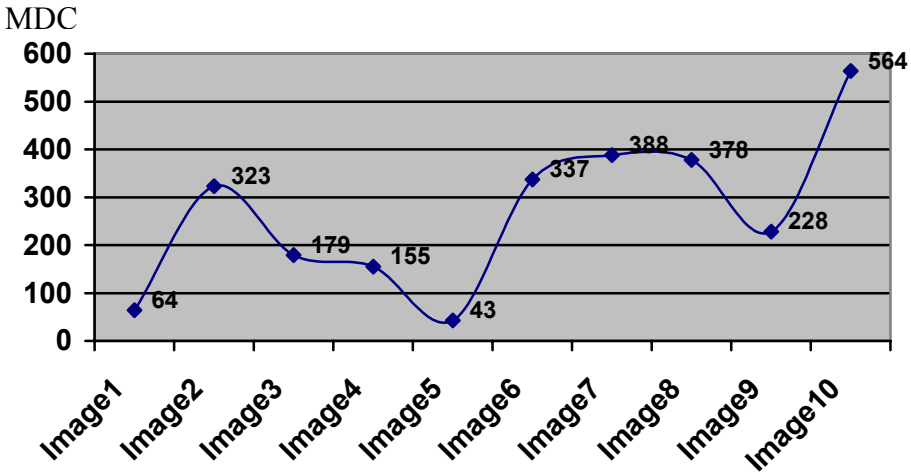

Image5

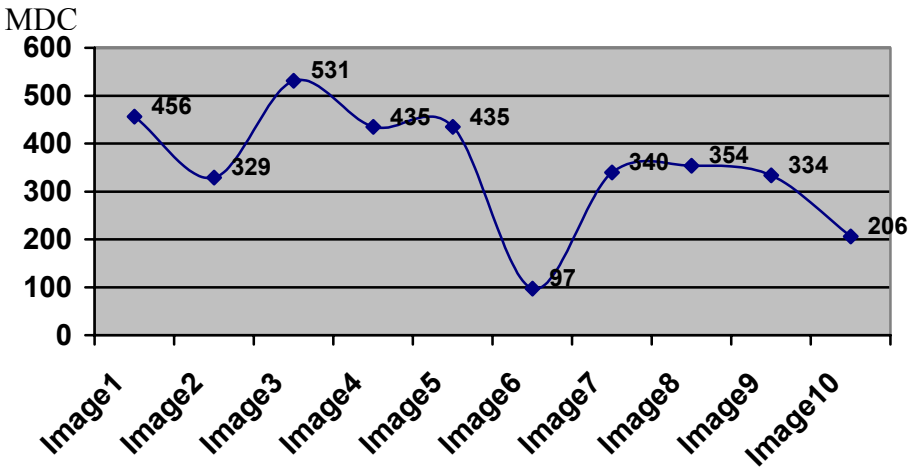

Image6

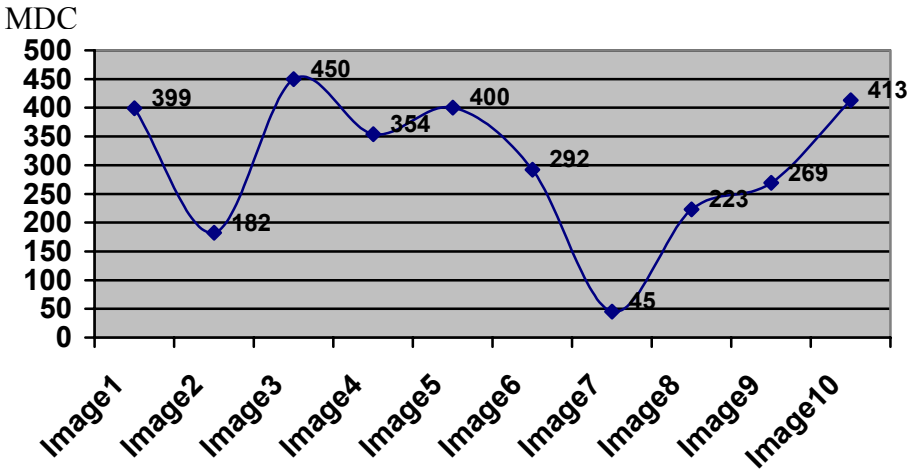

Image7

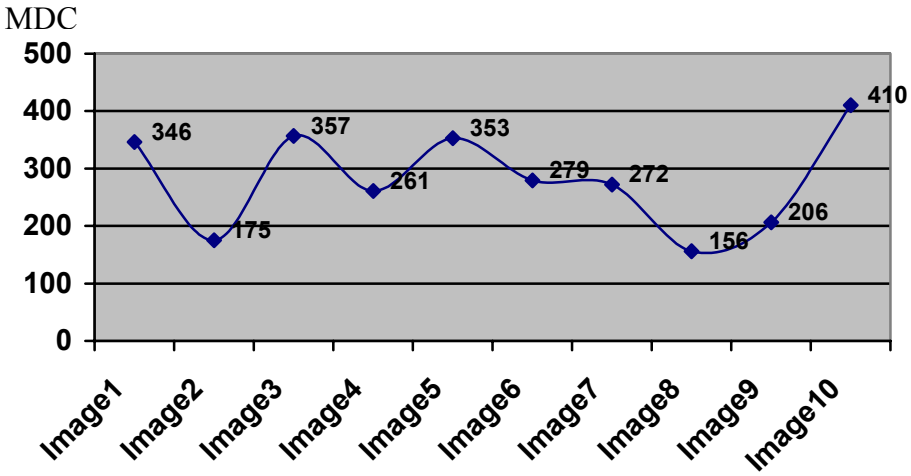

Image8

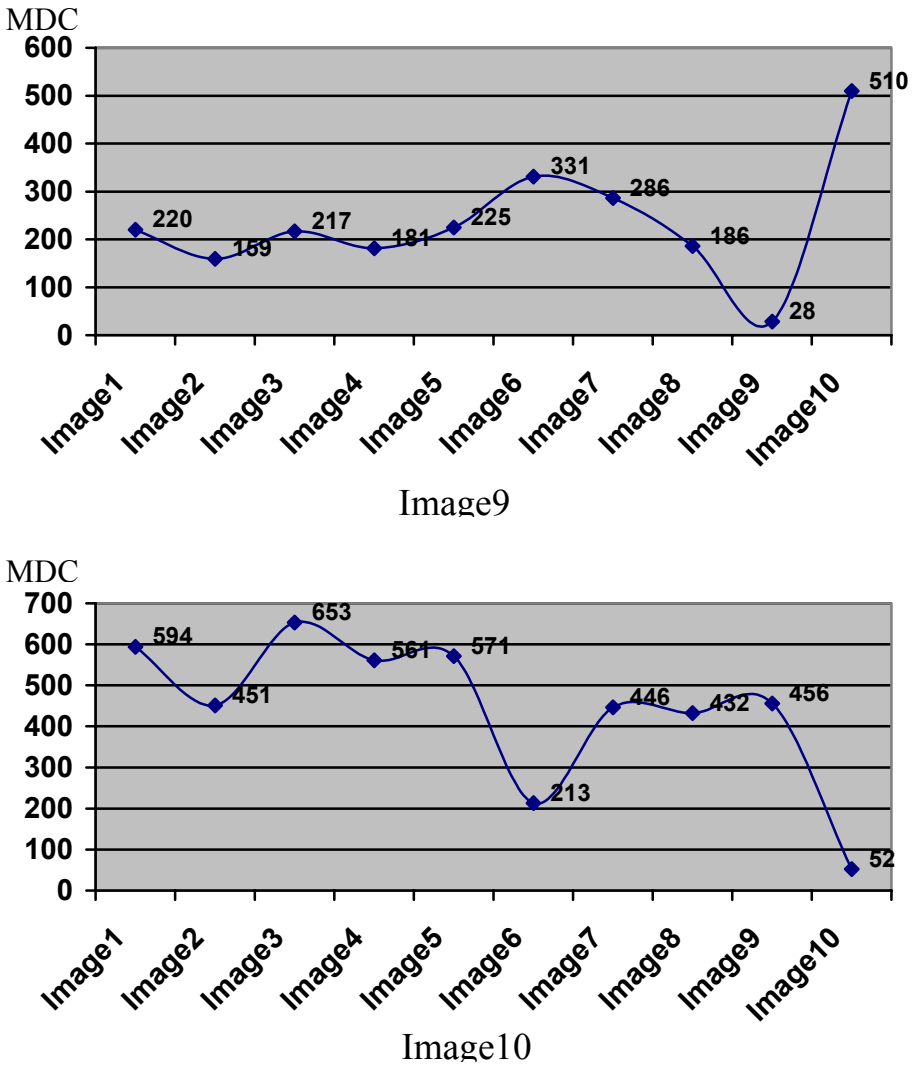

Figure (4.4) Illustrates the comparison of the rotated images with the database using Gabor filter alone

4.2 The Extracted Features

In this stage, Gabor filters have been used the differentiating the iris edge images into featured vector form, for each person in the database. Table (4.4) showing the extracted features of the images in the database using Gabor filters. Furthermore, Sobel gradient filters have been used, preceding the Gabor filter to globalize the image's edge features, shown in table (4.5).

The result of using Gabor filter alone has been found as to be copying better than utilizing the gradient Sobel filter with Gabor filters. This is accomplished by comparing the variances between different featured vectors; i.e. The Gabor results alone yield higher variance values between different persons. Figure (4.5) shows the difference of matching one person with the others that stored in the database, using Gabor filter only, and using both filters.

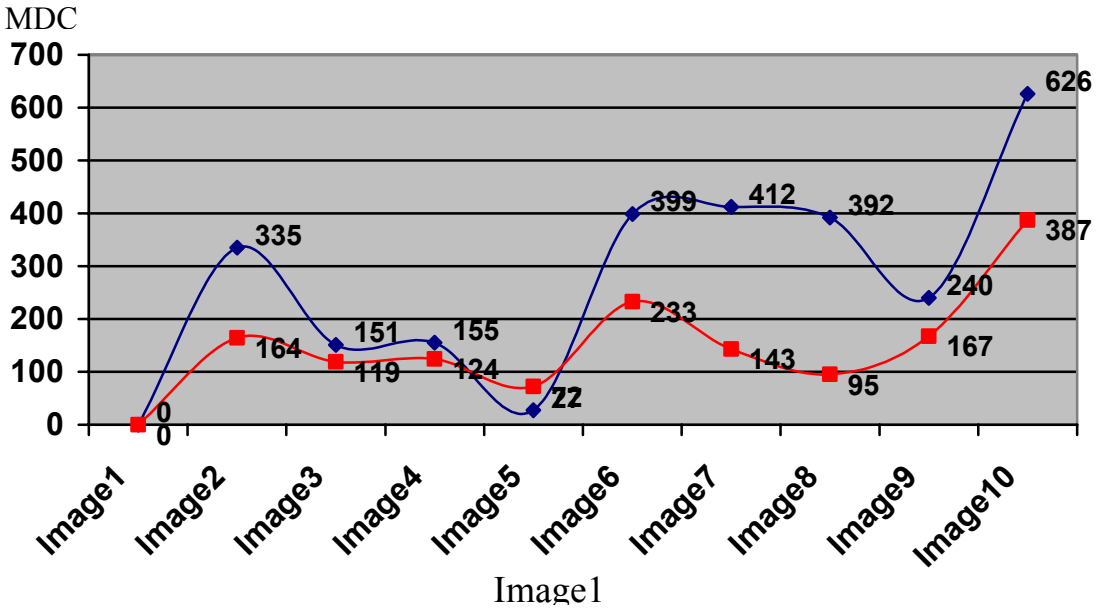

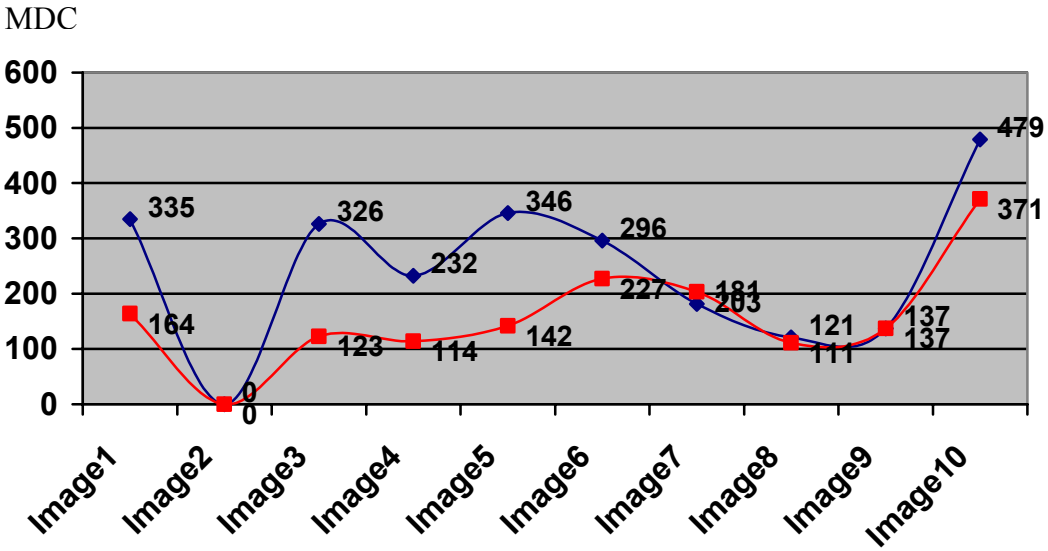

Image2

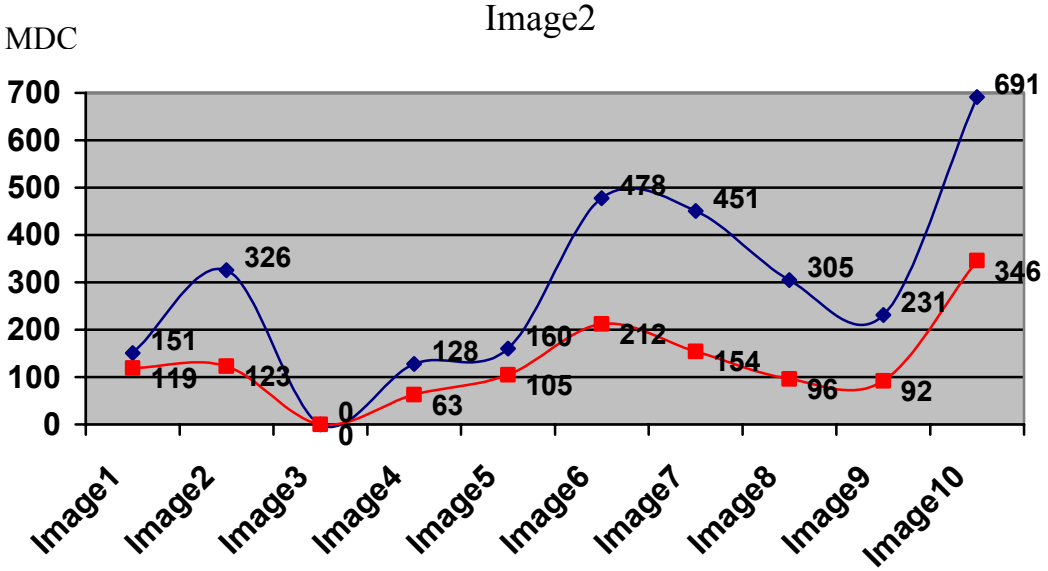

Image3

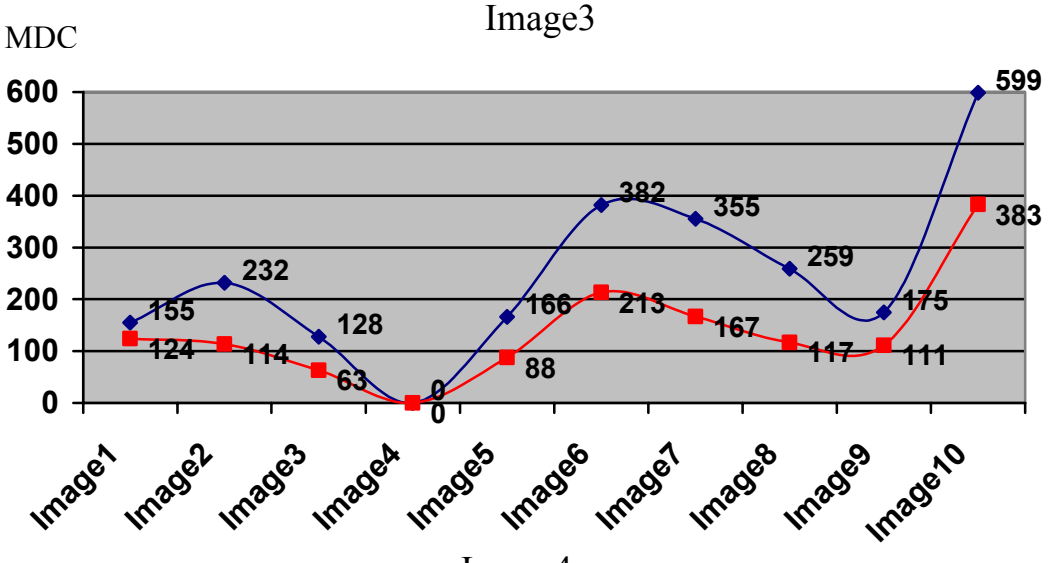

Image4

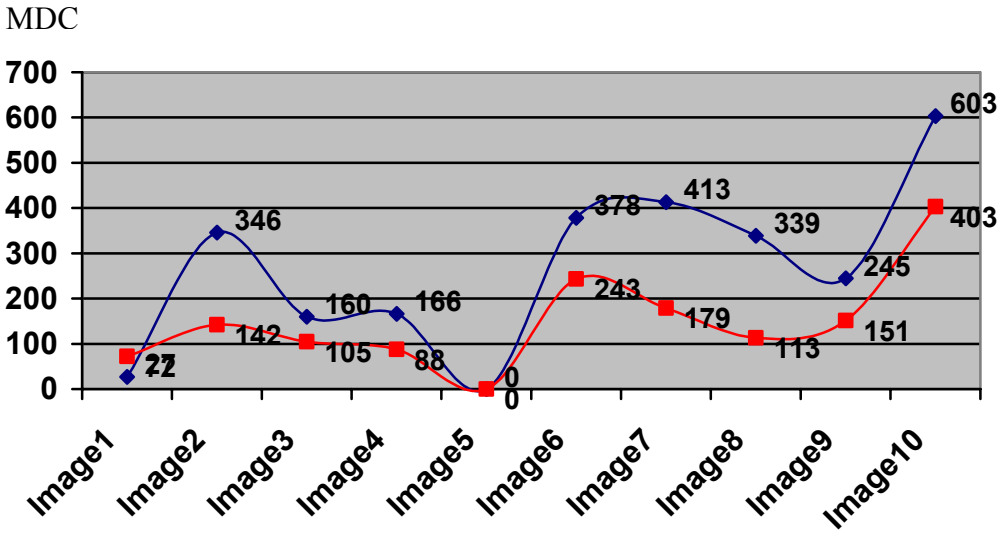

Image5

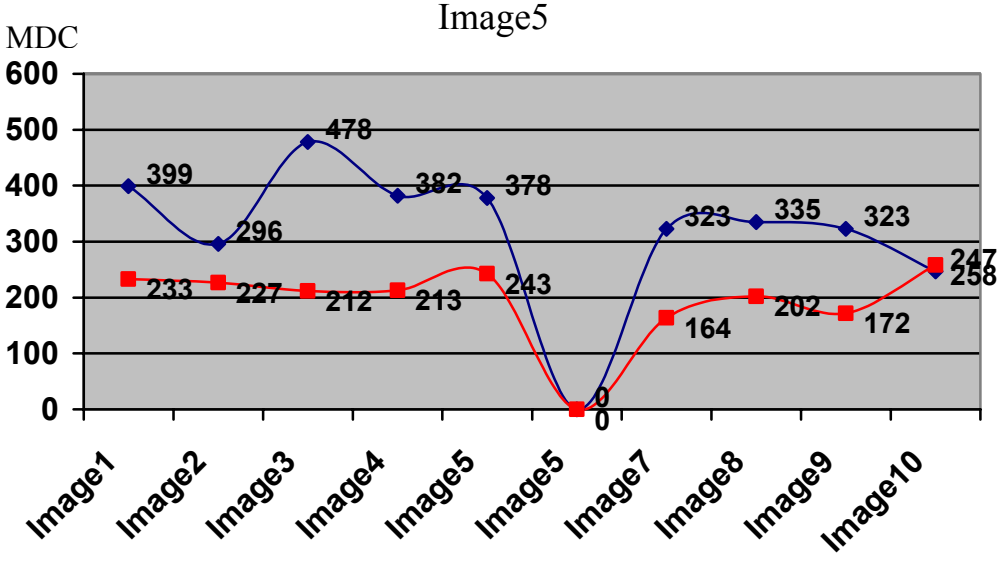

Image6

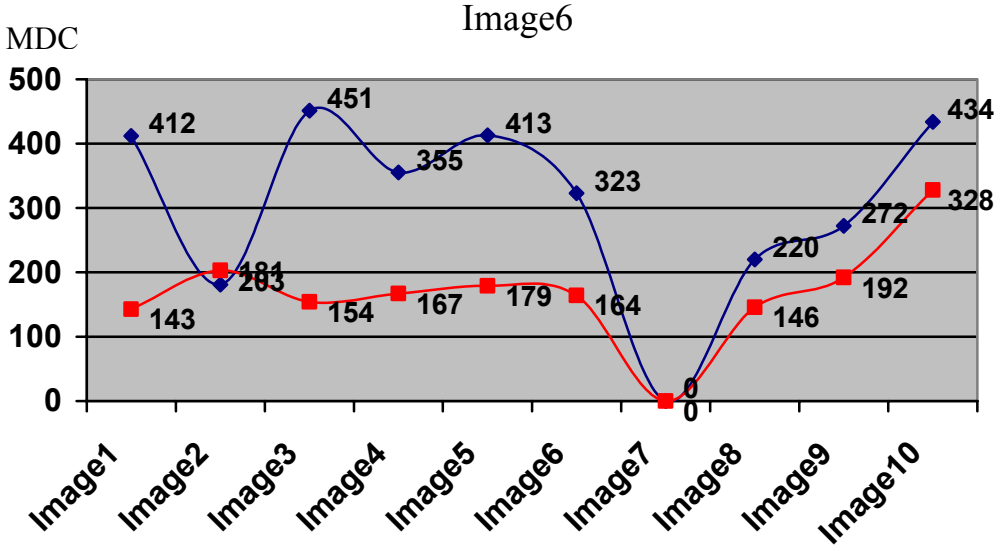

Image7

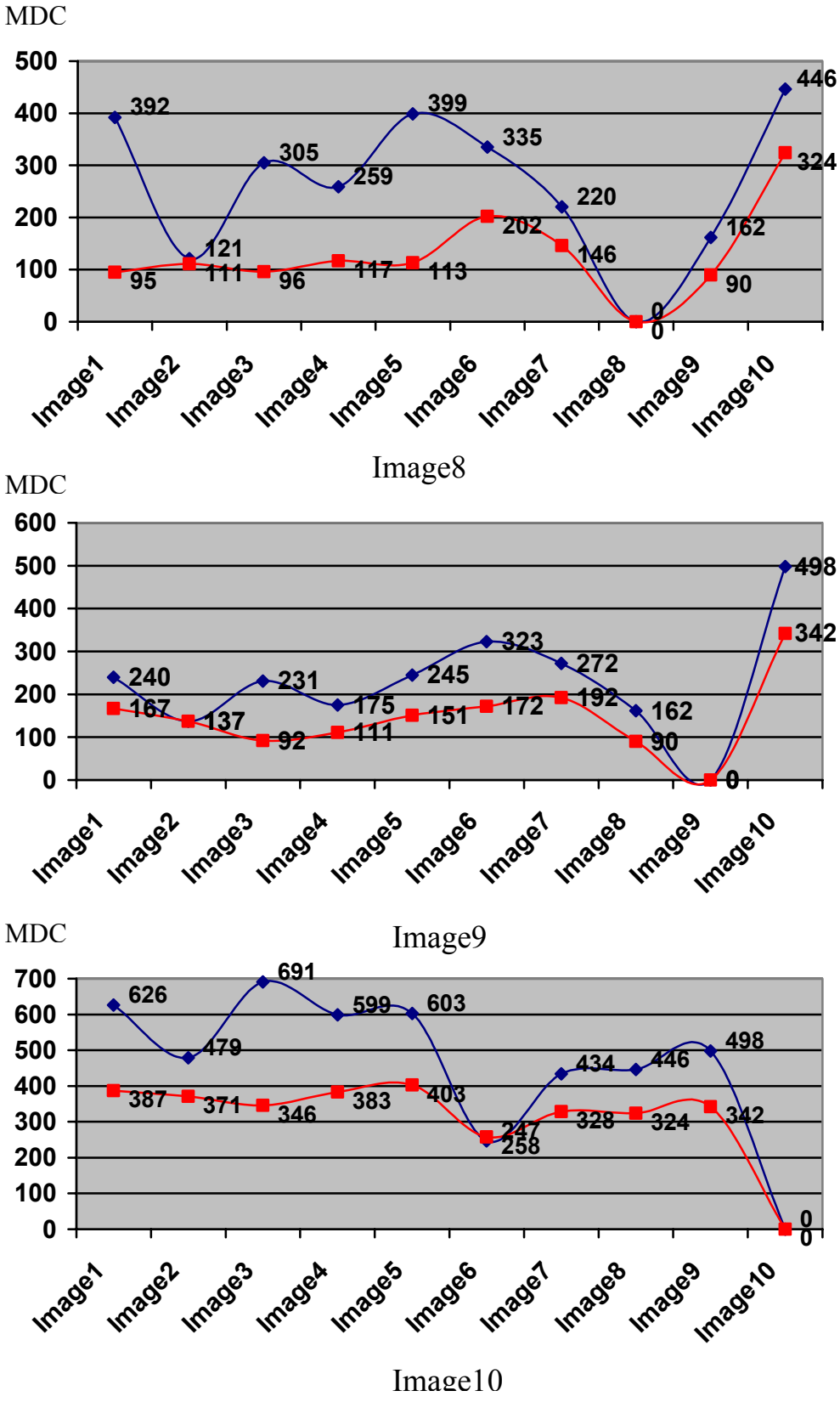

Figure (4.5) Illustrate the charts of implementing the given filters

Table (4.4) IrisCode feature vector using Gabor filter alone

feature vector	Image1	Image2	Image3	Image4	Image5	Image6	Image7	Image8	Image9	Image10
V(1)	72.47	50.29	74.22	74.07	71.09	47.8	43.45	51.39	54.29	42.34
V(2)	86.49	61.25	82.94	85.55	84.88	60.86	55.57	58.88	61.25	52.65
V(3)	90.62	63.09	83.78	86.57	88.78	67.62	59.19	60.12	62.23	59.11
V(4)	92.52	61.61	83.66	86.23	90.78	69.81	60.94	60.97	62.56	64.05
V(5)	91.7	57.13	83.22	86.1	89.54	69.88	63.03	61.36	61.27	66.86
V(6)	38.14	28.99	21.69	29.72	41.96	55.94	34.87	22.97	32.39	57.6
V(7)	14.77	12.28	12.72	13.68	14.86	26.29	10.18	14.98	14.93	42.83
V(8)	15.61	11.67	13.82	14.77	15.51	15.83	9.22	15.46	16.9	20.68
V(9)	13.86	12.39	15.04	15.59	14.16	13.71	10.09	15.9	17.14	14.94
V(10)	14	17.48	13.95	15.18	13.73	13.58	10.92	17.54	16.92	13.58
V(11)	21.59	19.43	13.41	16.95	23.13	37.85	25.11	13.55	19.07	37.5
V(12)	6.03	6.72	5.59	5.77	6.32	19.26	7.17	7. 55	6.22	27.79
V(13)	6.74	5.64	6.82	6.81	6.86	9.9	4.74	8. 23	7.42	15.33
V(14)	5.73	7	7.89	7.72	5.92	7.46	5.77	9.21	7.98	9.69
V(15)	5.39	11.34	7.69	8.04	5.24	7.02	6.15	10.08	7.99	7.49
V(16)	36.07	31.18	22.53	27.85	39	50.71	31.55	23.65	31.36	57.64
V(17)	14.51	14.49	13.36	13.46	14.73	25.29	10.48	15.23	15.06	41.94
V(18)	15.34	13.16	14.43	14.25	15.79	15.31	8.8	15.85	17.21	22.77
V(19)	13.69	13.77	15.68	15.32	14.18	13.45	9.71	15.95	16.58	16.42
V(20)	13.66	18.43	14.46	14.98	13.63	13.43	10.13	17.1	16.57	14.17
V(21)	69.3	53.63	78.54	62.38	69.1	45.14	37.83	49.73	65.62	39.46
V(22)	83.92	64.91	87.61	72.68	84.09	61.06	54.47	57.44	77.09	50.59
V(23)	86.92	67.15	88.36	73.52	87.12	66.94	55.37	58.67	77.78	56.24
V(24)	88.87	65.39	88.18	73.21	89.01	68.28	56.8	59.18	78.18	60.36
V(25)	88.34	60.35	87.95	73.29	88.34	69.23	58.57	59.54	76.67	61.76
V(26)	35.93	31.53	23.09	26.39	38	46.73	33.83	23.8	28.85	57.23
V(27)	14.53	14.92	13.73	12.71	14.35	23.32	10.75	15.23	14.42	41.65
V(28)	15.17	13.29	14.76	13.73	15.43	14.52	9.45	15.67	15.63	22.83
V(29)	13.75	13.83	15.93	14.54	14.05	12.19	10.19	16.03	15.3	16.64
V(30)	13.59	18.74	14.76	14.21	13.31	11.99	10.57	16.85	15.46	14.12
V(31)	21.56	19.28	13.4	16.94	23.08	37.86	25.14	13.52	19.06	37.46
V(32)	6	6.65	5.6	5.79	6.29	19.29	7.22	7.55	6.18	27.78
V(33)	6.73	5.62	6.82	6.82	6.83	9.86	4.76	8.22	7.41	15.31
V(34)	5.71	6.97	7.9	7.74	5.89	7.46	5.8	9.21	7.96	9.66
V(35)	5.38	11.25	7.68	8.06	5.24	7.03	6.17	10.07	7.99	7.49
V(36)	39.54	30.46	23.44	29.97	43.04	52.43	33.88	23.91	31.1	58.27
V(37)	15.43	13.14	13.84	13.83	15.24	24.77	9.45	15.4	14.98	43.21
V(38)	16.04	12.29	14.95	15.25	15.76	15.34	9.03	16.18	16.23	21.15
V(39)	14.49	12.91	16.29	15.85	14.72	12.61	9.65	16.58	16.56	15.46
V(40)	14.53	18.46	15.1	15.38	14.14	12.55	10.4	17.8	16.45	13.76

Table (4.5) IrisCode feature vector using Sobel filter with Gabor filter

feature vector	Image1	Image2	3Image	Image4	Image5	Image6	Image7	Image8	Image9	Image10
V(1)	19.43	16.31	18.5	21.45	16.12	11.37	22.12	17.82	12.1	14.81
V(2)	10.19	9.05	9.02	8.94	8.7	9.33	12.35	10.02	7.2	13.58
V(3)	7.71	6.79	7.63	7.58	7.4	5.86	8.23	8.98	6.93	10.79
V(4)	6.73	6.17	7.6	7.38	6.04	5.73	8.14	7.15	5.87	7.15
V(5)	5.26	7.26	5.58	5.98	3.82	6.13	7.81	6.68	5.83	6.13
V(6)	46.3	27.42	30.51	32.59	37.97	31.47	39.55	38.99	35.53	31.49
V(7)	12.43	8.59	8.18	7.82	9.44	31.09	20.54	11.1	10.97	39.49
V(8)	8.98	6.56	7.28	7.32	7.78	8.94	7.28	10.58	11.43	19.99
V(9)	7.44	6.97	8.13	7.06	6.74	9.08	7.41	8.99	11.08	11.69
V(10)	6.56	10.37	6.15	5.78	4.35	8.85	8.71	9.32	9.91	8.31
V(11)	58.14	49.54	46.96	46.01	57.04	38.87	43.92	49.85	41.08	48.71
V(12)	15.58	15.34	9.85	9.19	11.86	36.36	26.58	15.37	9.31	52.98
V(13)	9.55	10.15	9.17	9.13	9.39	10.98	6.05	11.89	11.58	34.29
V(14)	8.93	13.2	12.01	10.34	9.3	8.82	7.24	10.9	11.39	14.8
V(15)	7.72	22.62	9.65	8.46	6.06	9	9.04	11.87	10.46	9.87
V(16)	35.74	27.16	24.58	26.58	31.85	23.02	30.39	32	25.48	25.39
V(17)	11.47	9.82	7.2	7.15	9.11	18.83	15.25	10.29	7.99	25.7
V(18)	8.23	7.42	6.4	6.77	7.97	7.04	6.22	9.53	9.28	15.4
V(19)	7.05	7.89	7.23	6.83	6.65	6.98	6.73	8.06	8.63	9.11
V(20)	6.11	10.77	5.61	5.56	4.39	7.42	7.5	8.22	8.12	6.95
V(21)	24.89	16.79	24.96	17.69	18.89	19.87	26.91	26.85	22.85	19.76
V(22)	10.58	8.24	10.84	6.16	8.66	20.2	13.62	12.39	11.97	23.72
V(23)	7.87	6.1	9.08	5.41	6.98	9.58	7.59	11.46	11.27	17.16
V(24)	6.4	5.64	9.04	5.02	5.56	9.94	7.62	8.75	9.55	10.63
V(25)	5.28	7.28	6.64	4.09	3.72	9.5	7.72	8.23	9.13	7.61
V(26)	35.19	26.18	28.62	30.4	32.04	20.18	37.08	27.89	21.27	25.02
V(27)	11.58	9.52	8.48	8.33	8.65	16.15	19.1	9.56	7.11	25.08
V(28)	8.16	7.07	7.68	7.62	7.72	6.24	7.65	8.06	7.78	15.06
V(29)	7.27	7.66	8.72	8.15	6.99	5.66	8.12	7.18	7.25	8.79
V(30)	5.97	10.6	6.41	6.45	4.33	6.2	8.58	7.11	6.82	6.81
V(31)	57.96	49.14	46.06	45.46	56.85	39.72	43.28	50.99	41.53	48.72
V(32)	15.49	15.22	9.66	9.08	11.8	37.18	26.16	15.56	9.39	53.01
V(33)	9.5	10.07	8.96	9.04	9.37	11.22	6	12.13	11.71	34.35
V(34)	8.89	13.06	11.76	10.2	9.26	9.06	7.16	11.11	11.54	14.83
V(35)	7.72	22.4	9.47	8.35	6.05	9.19	8.92	12.13	10.56	9.86
V(36)	41.85	28.19	37.73	31.11	38.71	22.84	38.81	31.53	28.05	31.71
V(37)	11.76	9.01	10.01	7.67	9.13	21.82	20.39	9.92	9.03	39.3
V(38)	8.26	6.77	9.28	7.1	7.72	6.58	7.05	8.44	9.33	19.93
V(39)	7.05	7.24	10.51	7.24	7.04	6.06	7.23	7.46	8.75	11.67
V(40)	5.71	11.04	7.5	5.71	4.35	6.15	8.12	7.42	7.59	8.27

Chapter Five

Conclusions and Future works

5.1 Conclusions

From the results obtained by performing this designed recognition and identification system, the following points may be considered for conclusion;

1. The iris edge detection method, using Marr-Hildreth edge technique is proposed a good results with an appropriate Gaussian standard deviation value (i.e. σ =3), which gives closed contours and single edges for the proposed contour following process.
2. The 8 Gabor filters which were used to globalize the extracted features is copying better than utilizing the gradient Sobel filter with Gabor filters; i.e. The Gabor results alone yield higher variance values between different persons.
3. An additional amount of noise added to the tested eye's images (i.e. Gaussian of α = 1.25 and variance = 100), and the rotated image with β = 1, the test proved that this system is still identifying and recognizing these images using Gabor filters.

5.2 Suggestions for Future Works

1. Measures the texture components of the tissue surrounding the pupil of the eye, rather than using STD method for adding more classification accuracy for the system.
2. An image de-noising technique, based on utilizing the wavelet transformation method, may be adopted and performed to enhance the tested images (i.e. remove the eyelash) before carrying out the edge and iris recognition operations.
3. Widening the adopted orientations of the Gabor filters would led to extra features to improve the matching process, but on the expense of the execution time.

References

1. [Ali05a] Ali M. Mohamed, **"Hand Identification Using Fuzzy-Neural"**, M.Sc thesis, College of Science, Al-Nahrain University, 2005.
2. [Ali05b] Ali A. Ibrahem, **"Fingerprints Recognition Using Gabor Filters"**, M.Sc thesis, College of science Baghdad University, 2005.
3. [Ani91] Anil K. Jain, and Farrokhnia, F. **"Unsupervised Texture Segmentation Using Gabor Filters"**, Pattern Recognition, vol. 24, no. 12, pp. 1167-1186, 1991.
4. [Ani00] Anil K. Jain, Robert P.W. Duin and Jianchang Mao, **"Statistical Pattern Recognition: A Review"**, IEEE Transactions on pattern analysis and machine intelligence, Vol. 22, No. 1, 2000.
5. [Bho04] Bhola R. Meena, and Phalguni Gupta, **"Personal Identification Based on Iris Patterns"**, Institute of Technology, India, 2004. www.cse.iitk.ac.in/report-repository/2004/btpreport_Y0097
6. [Chr00] Christel-loic Tisse, Lionel Martin, Lionel Torres, Michel Robert, **"Person Identification Technique Using Human Iris Recognition"**, France University de Montpellier, Proceedings of the 15th International Conference on Vision Interface, pp. 294-299, 2000.
7. [Csa07] Csaba zepesvari, **"Image Processing: Low-level Feature Extraction"**, University of Alberta, 2007. www.cs.ualberta.ca/~szepesva/CMPUT412/ip2
8. [Dau94] Daugman J., **"Introduction to Iris Recognition"**, IEEE Transactions on Pattern Analysis and Machine Intelligence, vol. 15, no. 11, pp. 1148-1161, 1994.

9. [Dau01] Daugman, J., and Downing, C., **"Epigenetic Randomness, Complexity, and Singularity of Human Iris Patterns"**. Proceedings of the Royal Society, Biological Sciences vol. 268, pp. 1737-1740, 2001.
10. [Dau04] Daugman J., **"How Iris Recognition Works"**, Proceedings of International Conference on Image Processing, IEEE Transactions. On circuits and systems for video technology, Vol. 14, no. 1, pp. 21-30, 2004.
11. [Dun95] Dunn D., and W.E. Higgins, **"Optimal Gabor Filters for Texture Segmentation"**, IEEE Transactions on Image Processing, vol. 4, no. 4, pp. 947-964, 1995.
12. [Dav04] David Carr, **"Iris Recognition: Gabor Filtering"**, The Connexions Project and licensed, 2004.
13. [Ger97] Gerald O. Williams, **"Iris Recognition Technology"**, Iridian Technologies, IEEE Aerospace and Electronics Systems Magazine, vol. 12, no. 4, pp. 23-29, 1997.
14. [Gon87] Gonzalez R.C., and Wintz P., "**Digital Image Processing"**, Second Edition, Addison-Wesley Publishing Company, 1987.
15. [Gon74] Gonzalez R.C., and Tou T.J, **"Pattern Recognition Principles"**, Reading Mass., Addison-Wesley Publishing Company, 1974.
16. [Har05] Harvey Rhody, and Chester F. Carlson, **"Image Feature Detection"**, Rochester Institute of Technology, 2005. www.cis.rit.edu/class/simg782/lectures/lecture_15/lec782_05_15
17. [Hib03] Hiba Zuher., **"Hand Geometry-based on Identity Authentication Method"**, M.Sc thesis, College of science, Al-Nahrain University, 2003.
18. [Hug06] Hugo Proenc, and Lu´ıs A. Alexandre, **"Iris Recognition: An Analysis of the Aliasing Problem in the Iris Normalization Stage"**,

Published in IEEE Proceeding of the International Conference on Computation Intelligence and Security (CIS). Guangzhou. China. vol. 2. pp. 1771-1774, 2006.

19. [Jam03] James Greco, David Kallenborn, Dr. Michael C. Nechyba, **"Statistical Pattern Recognition of the Iris"**, 2003. www.mil.ufl.edu/publications/fcrar04/fcrar2004_iris
20. [Jas03] Jason L. Mitchell, Marwan Y. Ansari and Evan Hart, **"Advanced Image Processing with DirectX 9 Pixel Shaders"**, ATI Research,2003. ati.amd.com/developer/shaderx/ShaderX2_AdvancedImageProcessing.
21. [Jes05] Jesse Horst, **"Iris Recognition: A General Overview"**, Journal of Student Research, 2005. www.uwstout.edu/rs/2006/7Horst
22. [Kas94] Kasem M., **"Region Matching Method Based on Extracting the Interior of Bounded Areas"**, M.Sc thesis, College of science, Baghdad University, 1994.
23. [Li04] Li Ma, Tieniu Tan, Dexin Zhang, Yunhong Wang, **"Local Intensity Variation Analysis for Iris Recognition"**, Institute of Automation, Chinese Academy of Sciences, vol. 37, no. 6, pp. 1287–1298, 2004.
24. [Li02a] Li Ma, Yunhong Wang, Tieniu Tan, **"Iris Recognition Using Circular Symmetric Filters"**, National Laboratory of Pattern Recognition, Institute of Automation, Chinese Academy of Sciences, vol. 2, pp. 414–417, 2002.
25. [Li02b] Li Ma, Yunhong Wang, Tieniu Tan, "**Iris Recognition Based on Multichannel Gabor Filtering**", Chinese Academy of Sciences, vol. 1, pp.279-283, 2002.

26. [Lib03] Libor Masek, **"Recognition of Human Iris Patterns for Biometric Identification"**, School of Computer Science and Software Engineering, the University of Western Australia, 2003.
27. [Pau04] Paul Robichaux, **"Motivation Behind Iris Detection"**, Connexions Project, 2004. cnx.org/content/m12488/latest/ - 12k
28. [Tai96] Tai Sing Lee, **"Image Representation Using 2D Gabor Wavelets"**, IEEE transactions on pattern analysis and machine intelligence, vol. 18, no. 10, 1996.
29. [Umb98] Umbaugh S. E., **"Computer Vision and Image Processing"**, Printic-Hell, 1998.
30. [Yin04a] Yingzi Du, Robert Ives, Delores Etter, Thad Welch, **"A New Approach to Iris Pattern Recognition"**, United States Naval Academy Annapolis, submitted to IEEE International Conference on Pattern Recognition (ICPR), 2004.
31. [Yin04b] Yingzi Du, Robert Ives, Delores Etter, Thad Welch, Chein-I Chang, **"A One-Dimensional Approach for Iris Identification",** Electrical Engineering Department, Dept. of Computer Science and Electrical Engineering, University of Maryland, 2004.
32. [Yon99] Yong Zhu, Tieniu Tan and Yunhong Wang, **"Biometric Personal Identification System Based on Iris Pattern"**, Chinese Patent Application, vol.6, no. 99, 1999.

جمهورية العراق
وزارة التعليم العالي والبحث العلمي
جامعة النهرين
كلية العلوم

تقنية تمييز قزحية العين لإثبات الهوية الشخصية بإستخدام مرشحات كابور

رسالة
مقدمة إلى كلية العلوم في جامعة النهرين كجزء من
متطلبات نيل درجة الماجستير في علوم الحاسبات

من قبل
اسماء احمد كمال الراوي
(بكالوريوس جامعة النهرين ٢٠٠٥)

باشراف
د. بان نديم ذنون

نيسان ٢٠٠٨ ربيع الاول ١٤٢٩

الخلاصه

في هذا العمل تم تمثيل تقنية تمييز وتعريف الشخص، استنادا على قزحية عينه. وهذه التقنية المقدمه تستعمل عددا من طرق معالجة الصور؛ مثل تحديد الحافة ، متابعة الخطوط ، تشفير السلسلة ، مرشحات كابور، تطبيع الصورة، إستخلاص الخصائص، الخ. حيث تم استخدام صور من نوع جي بيك وبحجم ٢٥٦×٢٥٦ نقطه تحول إلى الشكل الرمادي عن طريق حساب معدل حزم الالوان الأحمر، الأخضر، والازرق.

ان الصورة الرماديه الناتجه تحول الى حافات وحدود بإستعمال تقنيةِ مار هلدريث لتحديد الحافات بقيمة الإنحراف المعياري الملائمة لداله الكاوس (الانحراف المعياري = ٣). اما منطقة القرنيه فحددت بتطبيق طريقة متابعة الخطوط المقترحه التي اعتمدت على خوارزمية تشفير السلسلة.

تم استخدام ثمانية قنوات لمرشحات كابور مثلت (بزوايا مختلفة (°١٥٧.٥، °١٣٥، °١١٢.٥، °٩٠، °٦٧.٥، °٤٥، °٢٢.٥، °٠) ولفت مع صورة القزحيه المنتَزعة. ثم طبعت الصور المعممة الصفات الناتجه من إلتواء مرشحات كابور إلى القيم المتوسطه وقيمِ الخلاف المقترحه، بإستعمال طريقة التطبيع المقترحه.

إن الصفات ال ٤٠ المستخلصه من كل قزحيه، (ثمانية للصور المعممه وخمسه اشرطه مقطعه) تخزن في ملف قاعدة البيانات.

اما تعريف الشخص يمكن أن يستخدم لقزحية العين الجديدة، باتباع نفس الإجراءات (المذكوره اعلاه)، لكن بمقارنة الصفات ال ٤٠ المستخلصه مع المخزونه في ملف قاعدة البيانات. وان إختبار التعريف يعطي احد النتيجتين أما "معرف" أو "غير معرف" اعتمادا على تطابق عملية المقارنه التي نفذت بإستعمال اقل مسافة كمعيار استخدم في هذا البحث.

اما النتائج فقد اظهرت ان نتيجة إستعمال مرشحات كابور لوحدها أفضل مِنْ إستعمال مرشح سوبل مع مرشحات كابور؛ وبمعنى آخر، فان نتائج كابور لوحده هي الأعلى بين الأشخاص المختلفين. وان دقة التصنيف = ١٠٠% بإستخدام مرشح كابور لوحده، بينما دقة التصنيف = ٨٠% بإستخدام مرشح سوبل معه.

Republic of Iraq
Ministry of Higher Education
and Scientific Research
Al-Nahrain University
College of Science

Iris Recognition Technique for Personal Identification Using Gabor Filters

A Thesis Submitted to the College of Science, Al-Nahrain University as aPartial Fulfillment of the Requirements for The degree of Master of Science in Computer Science

By
Asmaa Ahmed Kamal Al-Rawi
(B.Sc. 2005)

Supervised By

Dr. Ban N. Thanoon

April 2008 **Rabye Al-Awal 1429**

بِسْمِ اللهِ الرَّحْمنِ الرَّحِيمِ

هَلْ يَسْتَوِي الَّذِينَ يَعْلَمُونَ
وَالَّذِينَ لا يَعْلَمُونَ

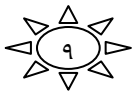

صَدَقَ اللهُ العَظِيمُ

الزمر

Supervisor Certification

I certify that this thesis is prepared under my supervision at the Department of Computer Science/ College of Science / Al-Nahrain University, By **Asmaa Ahmed Kamal Al-Rawi** as partial fulfillment of the requirements of the degree of Master of Science in Computer.

Signature:

Name: **Dr. Ban N. Thanoon**
Title: **Lecturer**
Date: **/ / 2008**

In view of the available recommendation, I forward this thesis for debate by the examining committee.

Signature:

Name: **Dr. Taha S. Bashaga**
Title: **Head of Department of Computer Science, Al-Nahrain University**
Date: **/ / 2008**

Examining Committee Certification

We certify, as an examining committee, that we have read the thesis titled **"Iris Recognition for Personal Identification Using Gabor Filters"**, presented by the student **Asmaa Ahmed Kamal Al-Rawi** and examined her in its content and what is related to it, and found that the thesis meets the standard for the degree of Master of Science in Computer.

Signature:

Name: **Dr. Laith Abdul Aziz Al-Ani**
Title : **Assist. Professor**
Date : **/ /2008**
(Chairman)

Signature:

Name: **Dr. Haithem A. Alani**
Title : **Lecturer**
Date : **/ /2008**
(Member)

Signature:

Name: **Dr. Amir S. Almalah**
Title : **Assistant Professor**
Date : **/ /2008**
(Member)

Signature:

Name: **Dr. Ban N. Thanoon**
Title : **Lecturer**
Date : **/ /2008**
(Supervisor)

Approved by the Dean of the Collage of Science, Al-Nahrain University.

Signature:

Name: **Dr. Laith Abdul Aziz Al-Ani**
Title : **Assist. Professor**
Date : **/ /2008**
(Dean of Collage of Science)

Dedicated To

My Dear Parents . . .

My Dear Husbend . . .

My Lovly Sisters . . .

For Their support and Help

And to every one gave me help and advise . . .

Asmaa

Acknowledgment

At first, I thank our God for helping me to complete this thesis.

I would like to express my sincere appreciator to my supervisor. ***Dr. Ban N. Thanoon*** *for giving me the major steps to go on to explain the subject. Sharing with me the ideas in my research "Iris Recognition Using Gabor Filters" and discuss the points that I felt they are important.*

Grateful thanks for the Head of Department of Computer Science. ***Dr. Taha S. Bashaqa****.*

Also I wish to thank the staff of Computer Science Department at ***Al-Nahrain University*** *for their help.*

I would like to say "thank you" to my faithful friends for supporting and giving me advises, and to my family and my dear husband.

Asmaa

Abstract

In this work, an identifying and recognizing person technique is presented based on its eye's iris. The introduce technique utilizes several image processing methods; e.g. edge detection, contour following, chain coding, Gabor filters, image normalization, feature extraction, etc. JPEG images of size 256×256 pixels are converted into grayscale form by averaging their Red, Green and Blue bands.

The produced grayscale image then traced into edges and boundaries using Marr-Hildreth edge technique with an appropriate Gaussian standard deviation value (i.e. σ =3). Iris region is detected by performing a suggested contour following method which is based on the chain coding algorithm.

Eight Gabor's filtering channels are simulated (with different orientations; $0^o, 22.5^o, 45^o, 67.5^0, 90^o, 112.5^o, 135^o$, and 157.5^o) and convolved with the iris's extracted image. The feature's globalized images produced from the Gabor filters convolution then, normalized to suggested mean and variance values, using a suggested normalization method.

A total of 40 features; (eight globalized images, and five for the sliced sectors), are stored in a created database file.

Person identification can then carried out, for new eye's iris, by following the same procedures (mentioned above), but comparing his or her extracted 40 features with those already preserved in the database file. The test of identification results in either "*Identified Person*" or "*Undefined Person*" depends on the similarity matching operation which carried out by utilizing the Minimum-Distance Classifier "*MDC*" criterion adopted in this research.

The result of using Gabor filters alone has been found as to be copying better than utilizing the gradient Sobel filter with Gabor filters; i.e. The Gabor results alone yield higher variance values between different persons. The classification accuracy = 100% using Gabor filters alone, while the classification accuracy = 80% using Sobel filter with Gabor filters.

Table of Contents

List of Abbreviations

Abbreviations	Meaning
1D	1 Dimension
2D	2 Dimensions
AAD	Average Absolute Deviation
DN	Discrete Numbers
FT	Fourier Transform
FFT	Fast Fourier Transform
IFFT	Inverse Fast Fourier Transform
ID	Identified person
IRS	Iris Recognition System
JPEG	Joint Photographic Experts Group
LoG	Laplacian of Gaussian operator
MDT	Minimum Distance Test
MDF	The Minimum value of MDT (Threshold value)
NFL	Nearest Feature Line
RGB	Red, Green, Blue, color bands
STD	Standard Deviation
Thr	Threshold value

List of Symbols

Symbol	Meaning
$\otimes$	Convolution operation
σ	The standard deviation of Gaussian function
$\frac{\partial}{\partial x}$	$\frac{d}{dx}$ Partial derivatives of
∇	First derivative of Laplacian operator
∇^2	Second derivative of Laplacian operator
$G\nabla^2$	Laplacian and Gaussian operator
α	A dummy variable of integration
$\Im$	The fourier transform
$\Im^{-1}$	Inverse fourier transform
$)\bar{y},\bar{x}($	The pupil core-point coordinates
$R_{Average}$	The pupil-radius
f	The frequency of the sinusoidal plane wave
θ	The 8 different orientation of Gabor filters
$\delta_{y'}$, $\delta_{x'}$	Standard deviations of the Gaussian envelope of Gabor filter
M_i , V_i	The estimated mean and variance values
M_0 , V_0	The proposed mean and variance values
(x, y)	Cartesian presentation
$)\theta($r,	Polar form